



# Detrital zircon record of Meso- and Neoproterozoic sedimentary basins in northern part of the Siberian Craton: Characterizing buried crust of the basement



Nadezhda Priyatkina<sup>a,b,\*</sup>, Andrei K. Khudoley<sup>b</sup>, William J. Collins<sup>a,c</sup>, N.B. Kuznetsov<sup>d,e,f</sup>, Hui-Qing Huang<sup>a</sup>

<sup>a</sup> New South Wales Institute of Frontiers Geoscience, University of Newcastle, Newcastle, NSW 2308, Australia

<sup>b</sup> Institute of the Earth Sciences, St. Petersburg State University, 7/9 University Nab., St. Petersburg 199034, Russia

<sup>c</sup> Department of Applied Geology, Curtin University, GPO Box U198, Perth, WA 6845, Australia

<sup>d</sup> Geological Institute, Russian Academy of Sciences, Pygeevsky 7, Moscow, Russia

<sup>e</sup> Gubkin Russian State Oil and Gas University, Leninsky per 65, Moscow, Russia

<sup>f</sup> Institute of Physics of the Earth, Russian Academy of Sciences, Bol. Gruzinskaya 10, Moscow, Russia

## ARTICLE INFO

### Article history:

Received 15 March 2016

Revised 19 July 2016

Accepted 1 September 2016

Available online 10 September 2016

### Keywords:

Siberian Craton

Western margin

Anabar

Meso- Neoproterozoic

Detrital zircon geochronology

Buried basement

## ABSTRACT

We present new LA ICP-MS detrital zircon data from Meso- and Neoproterozoic sedimentary basins located in the northern and western parts of the Siberian Craton. Along the western cratonic margin (Turukhansk Uplift, northern Yenisei Ridge), the basins accumulated predominantly 2.6–2.5 Ga and 1.9–1.85 Ga erosional products, while the main sources for the fill of intracratonic basin to the northeast near the Anabar Shield (East Anabar basin) were 2.9–2.7 Ga and 2.1–1.95 Ga old igneous rocks. The studied Meso- to Early Neoproterozoic sandstones were deposited in rift-related or passive margin settings, and underwent major craton-wide recycling to produce late Ediacaran siliclastic successions. Meso- to Early Neoproterozoic sandstones are immature to submature pointing to erosion of proximal Archean and Paleoproterozoic crustal units. The unique detrital age spectra for the northeast and western basins indicate provinciality and provide a basis for unravelling the age of buried domains of the Siberian Craton basement.

© 2016 Elsevier B.V. All rights reserved.

## 1. Introduction

The Siberian Craton (SC) is the largest Precambrian tectonic unit of Asia and comprises the rocks of Archean to Paleoproterozoic age (Glebovitsky et al., 2008; Rosen, 2002; Rosen et al., 1994). It is overlain by up to 12 km thick platform cover (e.g. Bazanov et al., 1976; Cherepanova et al., 2013; Nikishin et al., 2010), of which a significant part is represented by sedimentary units of Meso- to Neoproterozoic age (e.g. Frolov et al., 2015; Khudoley et al., 2007; Pisarevsky and Natapov, 2003). Based on stratigraphic correlations and seismic data interpretations, several Meso- and Neoproterozoic depositional basins have been identified (Surkov and Grishin, 1997; Melnikov et al., 2005; Frolov et al., 2015). Provenance studies of the intracratonic basinal siliclastic deposits may provide important information about the age of buried basement

in different parts of the craton. Until present, the ages of the major tectonic units in the craton were only depicted from *in situ* dating of rocks exposed within the basement, including the Aldan and Anabar Shield (Fig. 1). However, only 30% of the craton is exposed. The remainder is hidden by younger sedimentary cover. Other assumptions about the age of the basement came from Nd model ages of crystalline (igneous and metasedimentary) basement rocks (e.g. Kotov et al., 2006; Rosen et al., 2000; Kovach et al., 2000; Rosen et al., 2006), which are often ambiguous and cannot be directly correlated with U-Pb ages of basement units.

Recent publications released large detrital zircon datasets in order to characterise the provenance of sedimentary basins located near the southern and eastern parts of the SC (e.g. Khudoley et al., 2015; Powerman et al., 2015). In contrast, provenance of sedimentary basins located near the western and northern parts of the SC remains an under-reported aspect and is the focus of this paper. This is examined through a detailed detrital zircon study of Meso- to Neoproterozoic sedimentary rock in the northern Yenisei Ridge and Turukhansk regions to the west, and the Anabar Shield to the northeast (Fig. 1).

\* Corresponding author at: New South Wales Institute of Frontiers Geoscience, University of Newcastle, Newcastle, NSW 2308, Australia.

E-mail addresses: [nadezhda.priyatkina@gmail.com](mailto:nadezhda.priyatkina@gmail.com), [nadezhda.priyatkina@uon.edu.au](mailto:nadezhda.priyatkina@uon.edu.au) (N. Priyatkina).

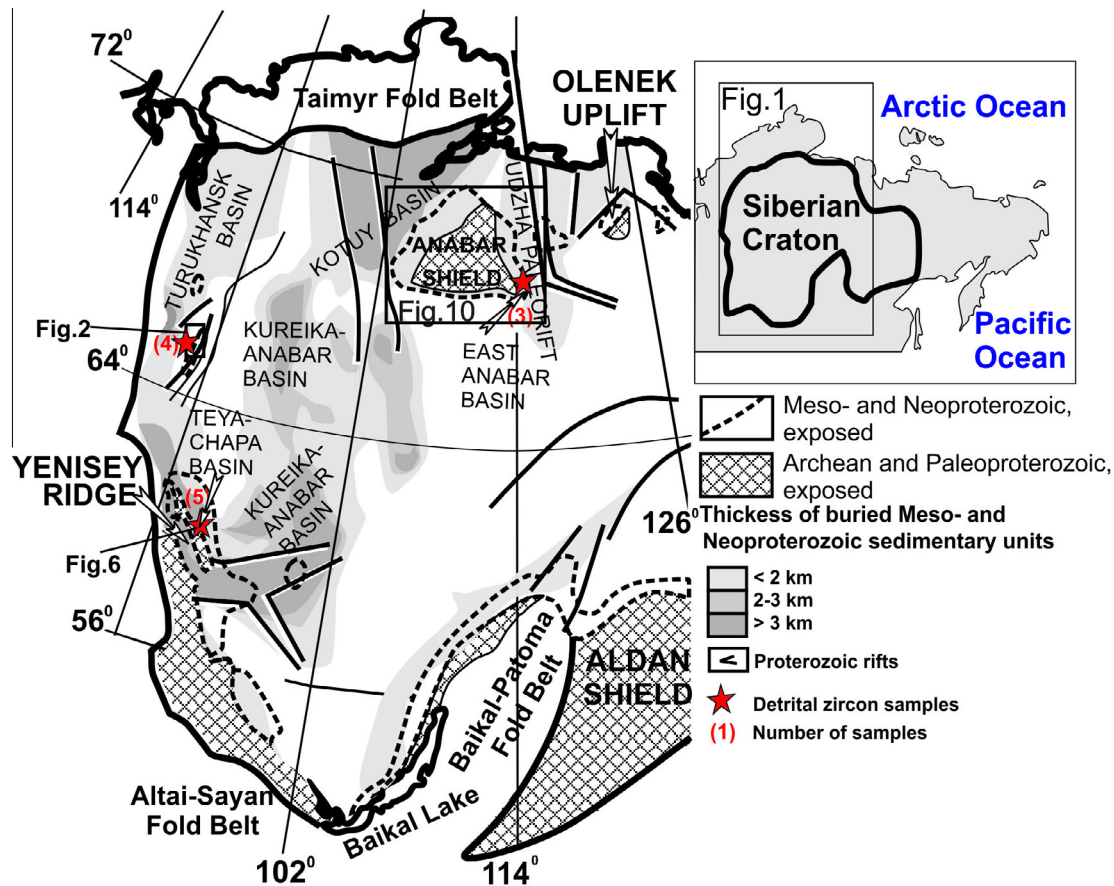


**Fig. 1.** Meso- and Neoproterozoic sedimentary cover of the Siberian Craton after Frolov et al. (2015) and Khudoley et al. (2007), and location of samples collected for detrital zircon study.

## 2. Meso- to Neoproterozoic sedimentary basins of the Siberian Craton

Meso- to Early Neoproterozoic and Ediacaran sedimentary units of the SC broadly form two distinct sedimentary successions separated by a major unconformity, defined by seismic and geological data (e.g. Frolov et al., 2015; Melnikov et al., 2005; Sovetov et al., 2007; Vernikovskiy et al., 2004). The unconformity is inferred to represent a hiatus, which lasted for 200 My and locally for up to 400 My (Gladkochub et al., 2009b). Pre-unconformity Meso- and Neoproterozoic sedimentary rocks were deposited in shallow-marine to fluvial environments and are widely distributed along the SC margins and within rift-related, intracratonic sedimentary basins (Frolov et al., 2015; Melnikov et al., 2005; Semikhatov and Serebryakov, 1983, see Fig. 1). Locally, sedimentary rocks host mafic sills and dyke swarms including the  $1384 \pm 2$  Ma Chieress dike (Ernst et al., 2000),  $1473 \pm 24$  Ma sill of the Olenek Uplift and  $1513 \pm 51$  Ma Fomich sills (Veselovskiy et al., 2006). Above the unconformity near the western cratonic margin, up to 2 km thick Ediacaran fluvial deposits of the Taseeva and Chapa groups make up a fill within a northerly trending set of foreland basins associated with the Neoproterozoic orogen of the Yenisei Ridge (Sovetov et al., 2007; Vernikovskiy et al., 2009). In the southwestern and southern margins of the SC, the Ediacaran rock units are represented by fluvial to near-shore clastic deposits of the Oselok Group and Ushakovka Formation. According to Sovetov et al. (2007) and Vernikovskiy et al. (2009), they represent a southern continuation of the foreland basins, whereas other researchers suggest their deposition in passive margin environments (Letnikova et al.,

2013; Pisarevskiy and Natapov, 2003). In the central and eastern parts of the platform, carbonate-dominated successions reflect deposition in an epicontinental sea, which covered nearly 90% of the SC during the Ediacaran.

The study areas along the western edge of the Craton include the peripheral Meso- to late Neoproterozoic Turukhansk basin and the late Neoproterozoic Teya-Chapa basin (Fig. 1). We compare and contrast these basins with the East Anabar basin, which exemplifies one of the Meso- to Neoproterozoic intracratonic basins near the Anabar Shield.

## 3. Analytical procedures

LA-ICP-MS of zircon U-Pb analyses were carried out at the University of Newcastle (Australia) using a NWR UP-213 Nd:YAG laser ablation system, coupled with an Agilent 7700x ICP-MS. Spot selection was guided by CL and transmitted light imaging. Standard spot ablation was employed, and the spot size (25 and 40  $\mu\text{m}$ ) was fixed in any individual session. A repetition rate of 5 Hz was used for all analyses. Helium gas was used as the laser ablation carrier gas. A single analysis typically contains 1 s (2 Hz) pre-ablation, 30 s washout time, 30 s background and 50 s sample analyses. Unknown sample analyses were interspersed with zircon standards GJ-1, Mud Tank, and 91500. Instrumental drift was modelled using Lolite 2.5, similar to that described by Paton et al. (2010). GJ-1, with a  $^{207}\text{Pb}/^{206}\text{Pb}$  age of  $608.5 \pm 0.4$  Ma (Jackson et al., 2004), was used as the primary standard for data reduction. Mud Tank and 91500 were used as secondary standard for accuracy valuation. Mud Tank and 91500 analyses gave age results

within 1% of the TIMS ages of 732 Ma (Black and Gulson, 1978) and 1065 Ma (Wiedenbeck et al., 1995), respectively. Internal error is normally better than 1%. Excess error estimated by calculating the additional uncertainty for each analysis required to produce an MSWD of 1 for the primary standard is typically better than 3% and is propagated to every single analysis as the external error. Analyses with internal errors greater than 3% and propagated errors greater than 5% have been excluded as they most likely reflect heterogeneous isotope ratios of zircons. In Appendix Table 1, we present both internal and propagated errors ( $2\sigma$ ).  $^{206}\text{Pb}/^{238}\text{U}$  ages are used when grains are younger than 1000 Ma. Otherwise,  $^{207}\text{Pb}/^{206}\text{Pb}$  ages are used as the best estimation of the age of zircon crystallization. U–Pb Concordia diagrams and age probability distribution plots have been prepared using ISOPLOT 3.0/EX (Ludwig, 2003). For constructing age probability distribution plots and further interpretation analyses with discordance greater than 10% were filtered, as well as grains with  $2\sigma$  error higher than 10%. Age peaks were calculated using Age Peak macro of Gehrels (2009). For each sample we present two values of maximum depositional age (MDA), calculated using two different methods suggested by (Dickinson and Gehrels, 2009). These include (1) youngest single grain (YSG) age, and (2) a more conservative estimate based on mean age of the youngest cluster ( $n \geq 3$ ) of grain ages that overlap in age at  $2\sigma$ , further referred to as mean age of the youngest cluster.

## 4. Turukhansk basin

### 4.1. Stratigraphy and sedimentological evolution

The 120 km long and 10–20 km wide Turukhansk Uplift (Fig. 2a) is made up of three fault-bounded tectonic blocks that preserve a >4.5 km thick succession of Meso- to Neoproterozoic carbonate and siliclastic deposits thrust eastwards along the western margin of the SC (Petrov and Semikhatov, 2001, 2009). The succession is folded into gently west-dipping monoclines, and a syncline with a gentle west limb and steep to overturned east limb (central Turukhansk block). These rock units are unconformably overlain by the Ediacaran–Cambrian platform cover succession.

The pre-Ediacaran Meso- to Neoproterozoic sedimentary sequence reflects growth of a carbonate platform (e.g. Petrov and Semikhatov, 2001). The sequence can be subdivided into two major siliclastic–carbonate cycles represented by the Kamensk and Nizhnetungusik groups separated by an erosional surface (Petrov, 2006; see also Fig. 2b). The Kamensk Group commences with >950 m thick Bezymenskaya Formation (=Strelnye Gory Formation by Frolov et al., 2015) that is dominated by alternating cross-bedded subarkosic sandstones, siltstones, and shales. Depositional environments varied from deep shelf-basin to above-wave base on a N–NW dipping continental shelf (Petrov, 1993). It is overlain by dominantly carbonate-clay 180–300 m thick Linok Formation, which consists of erosional products derived from proximal microbial mats (Petrov, 2000, 2001). The overlying 530–670 m thick Sukhaya Tunguska Formation consists of limestone and dolostones with intercalations of black cherts in its upper part (Petrov, 2011, and Ref. therein). The limestone yielded a Pb–Pb isochron age of  $1035 \pm 60$  Ma (Ovchinnikova et al., 1995) that remains the only direct geochronological constraint for the Turukhansk section. The upper siliclastic–carbonate sedimentary cycle includes the Derevninskaya (75–270 m), Burovaya (460–1000 m), Shorikha (620–700 m), Miroyedikha (150–210 m) and Turukhansk (up to 200 m) formations. They are predominantly stromatolite reef-bearing units with sandstone and shale interbeds which formed different parts of carbonate platform, although some shale units

were deposited in more deep-water environments below storm wave-base (Petrov and Semikhatov, 2009).

Based on paleontological and chemostratigraphic data (Gallet et al., 2000, and Ref. therein), the Derevninskaya and Burovaya formations have been correlated to Lower Lakhanda Group of the Uchur–Maya region located near the southeastern margin of Siberia. The Lakhanda Group underlies Uy Group, which in turn is cut by  $1005 \pm 4$  Ma mafic sills (U–Pb baddelyite; Rainbird et al., 1998) and has a Pb–Pb isochron carbonate age of  $1025 \pm 40$  Ma (Semikhatov et al., 2000). The age is also within error of that for the Sukhaya Tunguska Formation, and suggests the two could have been correlatives as well.

The post-unconformity Ediacaran–Cambrian sedimentary sequence commenced with the 200–400 m thick Platonovskaya Formation (Bartley et al., 1998), with a basal siliclastic layer represented by quartzose gravelstone and sandstone, followed upward by dolostone, marl and anhydrite-bearing limestone. In the Turukhansk Uplift, the dominantly carbonate sedimentation continued during the Early–Mid Cambrian when up to 1700 m thick limestone of the Kostinskaya Formation was deposited, followed by accumulation of the Mid–Late Cambrian carbonate-clayey Letninskaya (200 m) and Ust’-Pel’atinskaya formations (200 m).

### 4.2. Sample description and results of U–Pb detrital zircon dating

#### 4.2.1. Bezymenskaya Formation (sample NT-5)

The sample of the Bezymenskaya Formation is a light-grey sandstone with bimodal cross-bedding, collected from a riverbank outcrop on the Nizhnaya Tunguska River (Fig. 2, Attachment 1). Microscope study reveals that NT-5 is an arkose (Fig. 3a), consisting of alternating medium- to fine-grained laminae. Framework grains (90–95% of total thin section area) are moderately to well sorted and are typically subangular to subrounded monocrystalline quartz (70% of detrital grains) and feldspar, the latter partially replaced by kaolinite (30% of detrital grains). ~10% of quartz shows undulose extinction. Accessory minerals include biotite, zircon, and apatite. Cement (5–10%) consists of clayey material, locally with patches of an opaque phase.

Recovered zircons are 100–200  $\mu\text{m}$  long, colourless and pale yellow grains. Nearly 70% are prismatic subhedral to euhedral grains, and 30% are rounded. NT-5 had 99 detrital grains successfully analyzed, of which 72 meet 5% discordance criteria. The detrital zircon age spectrum of sample NT-5 is dominated by ca. 2520–2680 Ma population (79%), which defines a prominent peak at 2590 Ma (Fig. 5a). Accessory peaks are 2500 Ma (6%) and 2700 Ma (10%). Remaining grains are single Paleoproterozoic zircons with  $^{207}\text{Pb}/^{206}\text{Pb}$  ages of  $2286 \pm 31$  Ma,  $1904 \pm 35$  Ma and  $1786 \pm 26$  Ma. Mean age of the youngest cluster and the YSG ages are  $2490 \pm 14$  Ma ( $n = 3$ , MSWD = 0.34) and  $1786 \pm 26$  Ma respectively, significantly older than the age of sedimentation inferred from Pb–Pb isochron carbonate dating and stratigraphic correlations (Melnikov et al., 2005; Petrov, 1993, 2006).

#### 4.2.2. Derevninskaya Formation (NT-6/1)

Sample NT-6/1 was collected on the Nizhnaya Tunguska River near Strelnye Gory village, from a siliclastic package enclosed within the limestone-dominated Derevninskaya Formation (Fig. 2, Attachment 1). The sample is a light grey-colored quartz arenite with visible heavy mineral laminae. The framework (100% of total thin section area) consists almost solely of well-sorted, subrounded monocrystalline quartz grains (95%) that are 0.1–0.3 mm in diameter (Fig. 3b). 20% of quartz grains show undulose extinction. Minor components (<5%) are K-feldspar and 0.1–0.2 mm subrounded chlorite interlocked with brown aggregates of iron hydroxides to form intergranular patches. Zircon is present as an accessory mineral.



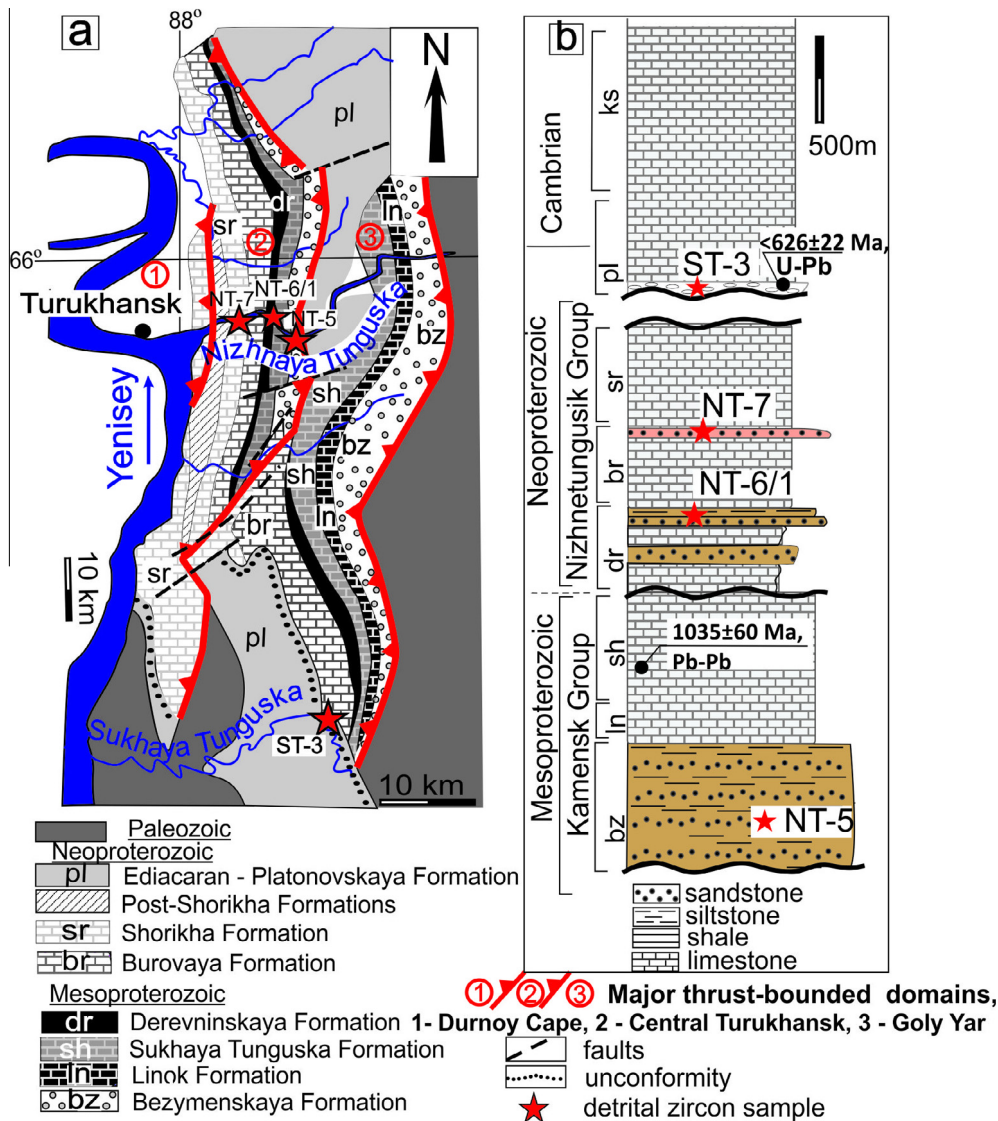


**Fig. 2.** Simplified geological map of the Turukhansk Uplift (a) compiled from Gallet et al. (2000), Petrov and Semikhatov (2001, 2009), and stratigraphy of the Turukhansk basin succession (b) after Petrov (2006) with detrital zircon sampling locations. Age estimate for Shorikha Formation is based on Ovchinnikova et al. (1995) and lower age limit for Platonovskaya Formation from this study.

The majority of recovered zircons are 70–150  $\mu\text{m}$  long, colourless and pale yellow. ~70% of the population are prismatic sub-rounded grains; ~30% are rounded.

NT-6/1 had 98 detrital grains successfully analyzed, of which 63 meet 5% discordance criteria (Fig. 5b). The predominant zircon population recovered from the sample is ca. 2600–2500 Ma (63%, mostly subrounded grains that commonly retain prismatic shape, Fig. 4a), that defines a prominent peak at ca. 2580 Ma (Fig. 5b). The older Archean grains are commonly rounded (see example on Fig. 4a) and make up the minor 2700–2600 Ma population (35%). The only significant Paleoproterozoic age group is ca. 1880–1850 Ma (13%, subrounded grains) that clusters at 1870 Ma. Single Paleoproterozoic grains with ages of ca. 1800 Ma, ca. 2150 Ma, ca. 2400–2300 constitute the remaining part of age spectrum. Maximum depositional age (MDA) based on mean age of the youngest cluster is  $1864 \pm 30$  Ma ( $n=3$ , MSWD = 0.2.9) and the YSG age is  $1803 \pm 13$  Ma. However, these grains are much older than the age of sedimentation obtained from the Pb-Pb isochron age and stratigraphic correlations (Melnikov et al., 2005; Petrov, 1993, 2006).

#### 4.2.3. Burovaya Formation (NT-7)

A dark brown, laminated, highly limonitized sandstone (sample NT-7) was collected from the very top of the Burovaya Formation near Glauconite Cape on Nizhnaya Tunguska River (Fig. 2, Attachment 1). Microscope study shows it is a fine-grained, calcarenaceous glauconitic quartz arenite (Fig. 3c). The rock consists of dark and light laminae with thickness of 1–4 mm. The framework (up to 100% of total thin section area) of light colored laminae consists of monocrystalline detrital quartz (25% of detrital grains), glauconite (35%) and calcite/dolomite (40%). Accessory phases concentrate in light-colored laminae and include zircon and opaque phase probably represented by magnetite altered to hematite. Dark laminae have lower content of monocrystalline detrital quartz (20%) and calcite/dolomite (25%), but higher content of detrital opaque minerals (15%), glauconite (40%) as well as trace amounts of zircon. Opaque minerals and zircon are angular to well rounded. Glauconite mostly forms subrounded pellets with diameter of 0.1–0.3 mm. A carbonate mineral phase forms 0.2–0.4 mm long crystals. Glauconite and carbonate (calcite/dolomite) sporadically form irregularly shaped aggregate (5%), cementing the framework.



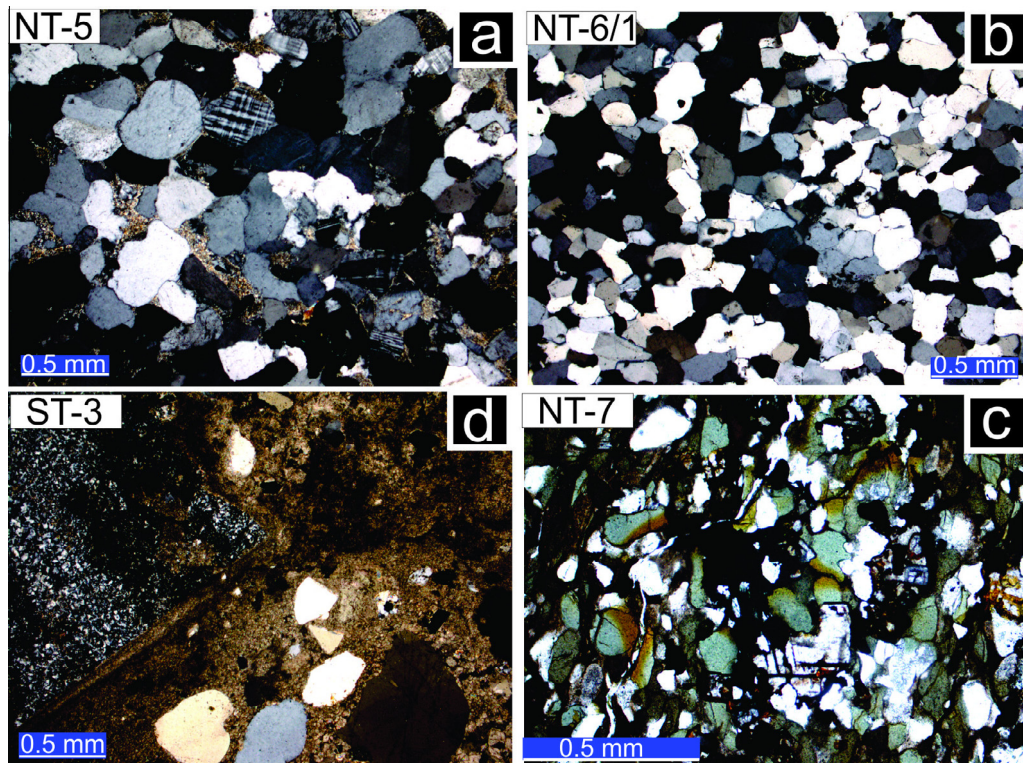


**Fig. 3.** Microphotographs of the representative thin-sections under cross polarized light (a, b, d) and parallel polarized light (c). The samples include: arkose sandstone of the Bezymenskaya Formation, (a), well sorted quartz arenite of the Derevninskaya Formation (b), poorly sorted glauconite sandstone from the top of Burovaya Formation (c) and calcareous conglomerate from the unconformity surface at the bottom of the Platonovskaya Formation (d).

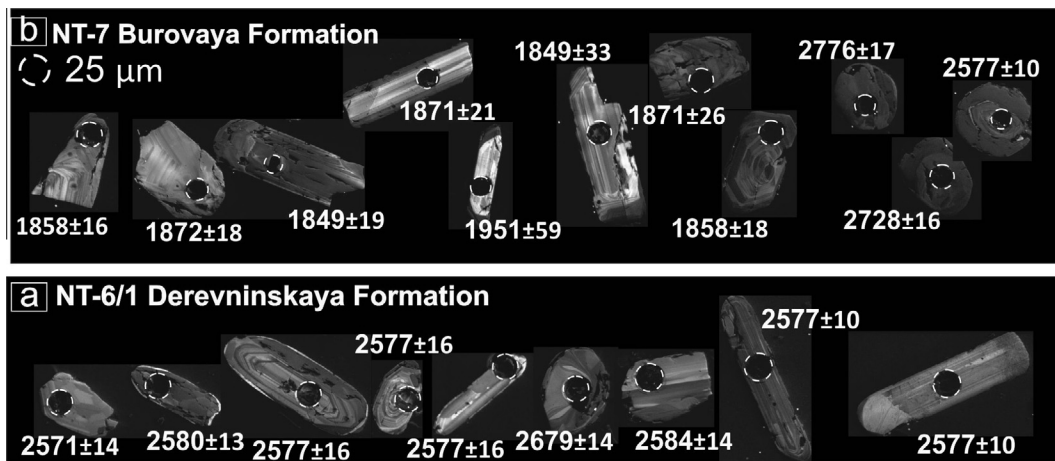


**Fig. 4.** Representative cathodoluminescence images of selected detrital zircon grains from samples NT-6/1 (a) and NT-7 (b).

The extracted heavy mineral concentrate contained abundant pyrite and other sulphides as well as a bimodal population of zircon. The zircon grains are 70–200  $\mu\text{m}$  long and  $\sim 50\%$  are well-shaped prismatic, while the other  $\sim 50\%$  are subrounded to rounded grains.

NT-7 had 102 successfully analyzed detrital grains, of which 93 meet 5% discordance criteria. Its detrital zircon age spectrum has a major peak at 1865 Ma (Fig. 5c) defined by predominant ca. 1820–1920 Ma population of zircons (57%). Some of them are perfectly euhedral grains, that preserve zoning (Fig. 4b). Minor Paleoproterozoic zircon populations (14%, commonly subrounded grains) define accessory peaks at 1945 Ma and

2030 Ma. In contrast to analysed samples from the lower units, earliest Paleoproterozoic and Neoproterozoic detrital zircons are abundant (30%) in sample NT-7. They are represented mostly by subrounded to rounded grains. Their ages define a nearly continuous 2900–2450 Ma signature, within which peaks at 2480 Ma, 2600 Ma, 2720 Ma, 2860–2880 Ma can be identified. The MDA determined based on mean age of the youngest cluster is  $1834 \pm 15$  Ma ( $n=3$ ,  $\text{MSWD}=0.08$ ) and the YSG age is  $1060 \pm 29$  Ma. The YSG age ( $1060 \pm 29$  Ma) overlaps within  $2\sigma$  the Pb–Pb isochron carbonate age of the Sukhaya Tunguska Formation ( $1035 \pm 60$  Ma) and seems to be the best estimate of sedimentation age.

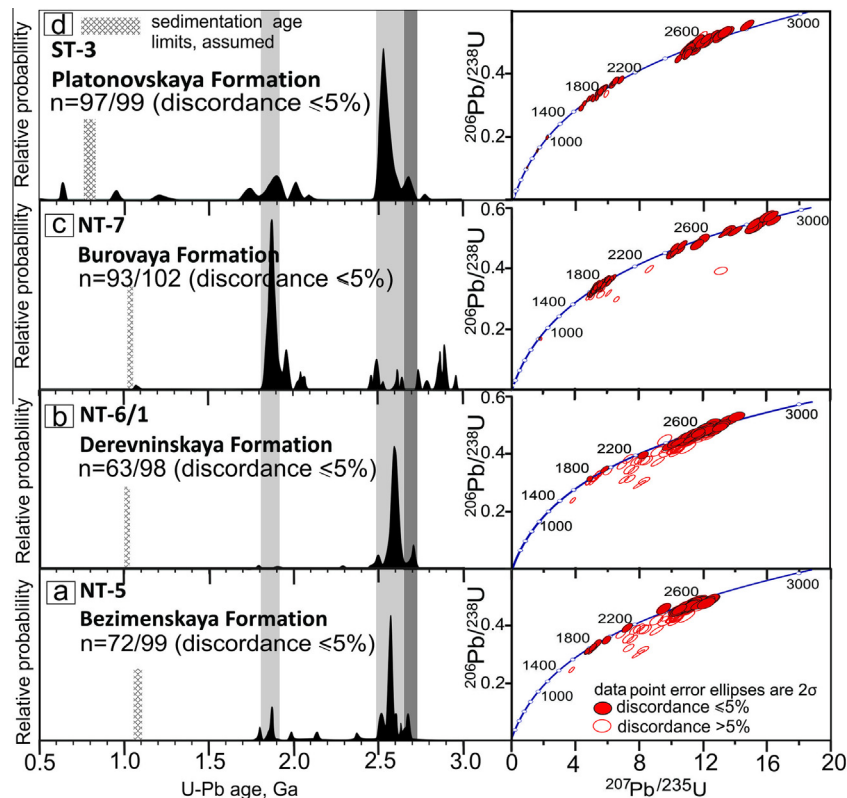


**Fig. 5.** Obtained age spectra of detrital zircon populations with related concordia plots (right hand side) from Bezimenskaya (a), Derevninskaya (b), Burovaya (c) and Platonovskaya (d) formations. For sedimentation age limits see references in text.

#### 4.2.4. Platonovskaya Formation (ST-3)

Sample ST-3 was collected directly above the unconformity between the Burovaya and Platonovskaya formations on the river-bank of the Sukhaya Tunguska River (Fig. 2, Attachment 1). The sample is from a 1 m thick package of conglomerate that contains fragments of the underlying stromatolite biogermes of the Shorikha Formation, as well as quartz gravel. Microscope study reveals that ST-3 is a calcareous litharenite (Fig. 3d). The framework (50%) consists of nearly equal proportions of monocrystalline quartz grains (50% of detrital grains), polycrystalline quartz (40%) and fragments entirely replaced by calcite/dolomite (<10%). Grains of monocrystalline quartz are mostly rounded, poorly sorted (0.05–0.7 mm in diameter), showing etching and embayment indicative of solution. Polycrystalline quartz constitutes angular fragments that are 0.3–30 mm long. Rare 1 mm diameter rounded fragments replaced by carbonate stand out of the carbonate matrix because of their finer granulation and a darker color compared to cement. Trace plagioclase, garnet and opaque minerals have been detected in thin-section. Cement (50%) is represented by a carbonate (calcite/dolomite) aggregate.

The zircons extracted from the sample are mostly colorless, clear rounded prisms with nearly equal size of 100–150  $\mu\text{m}$ . The sample ST-3 had 99 successfully analyzed detrital grains, of which 97 grains meet the discordance criteria. The detrital zircon age distribution pattern (Fig. 5d) broadly conforms to samples NT-5 and NT-6/1 (Fig. 5 a and b) and is characterized by a major age peak at 2530 Ma (60%). Ca. 2640–2700 Ma grains define an secondary Neoproterozoic peak at 2680 Ma (8%). The oldest zircon grain is 2775  $\pm$  28 Ma. Subordinate Paleoproterozoic grains are subdivided into a 1720–1800 Ma population that define a peak at 1750 Ma (5%), 1820–1940 Ma that defines a peak at 1900 Ma (12%) and 1980–2080 Ma (7%) that define a peak at 2020 Ma. Single Neoproterozoic grains have  $^{206}\text{Pb}/^{238}\text{U}$  ages of 632  $\pm$  17 Ma, 635  $\pm$  17 Ma,

938  $\pm$  24 Ma, 958  $\pm$  28 Ma and thus form two grain clusters that overlap at  $2\sigma$  level. Strict MDA determination based on mean age of the youngest cluster is 1730  $\pm$  21 Ma ( $n = 3$ , MSWD = 0.42), and based on YSG age is 632  $\pm$  17 Ma. The 630 Ma age agrees with an assumed late Ediacaran/Early Cambrian age of host rocks.

## 5. Teya-Chapa basin

### 5.1. Stratigraphy and sedimentary evolution

The Ediacaran/Early Cambrian Teya-Chapa basin is located in the northern part of the Yenisei Ridge (Fig. 1, Fig. 6a). The basin (Fig. 6b) is underlain by the metasedimentary Sukhopit Group (Postelnikov, 1980), which comprises an isoclinally folded package of quartzite (Fig. 6c) and quartz-sericite schist in its lower part, structurally overlain by phyllite and a flysch-like Pogor'uy Formation of sandstone and shale in the upper part. The rocks of the Sukhopit Group were intruded by ca. 880–860 Ma Teya granites (Nozhkin et al., 1999), metamorphosed and thrust onto the SC during the Neoproterozoic Baikalian orogeny (Vernikovskiy et al., 2003). Sukhopit's siliclastic units may represent the fragment of a continental slope of late Mesoproterozoic age as suggest K-Ar glauconite age estimates from the Group's uppermost Pogor'uy Formation (Volobuev et al., 1976).

Tectonic slices of Penchenga amphibolite facies rocks that occur in the region are commonly interpreted as late Paleoproterozoic (Nozhkin et al., 2010) or early Mesoproterozoic (Likhanov et al., 2008 and Ref. therein) basement to the Sukhopit Group (Likhanov et al., 2008; Nozhkin et al., 2010, 2012; Vrublevich, 1973). Nonetheless, the Penchnega rocks are spatially associated with the Korda Formation of the lowermost Sukhopit Group, and shows broadly similar structural trends and degree of metamorphism.



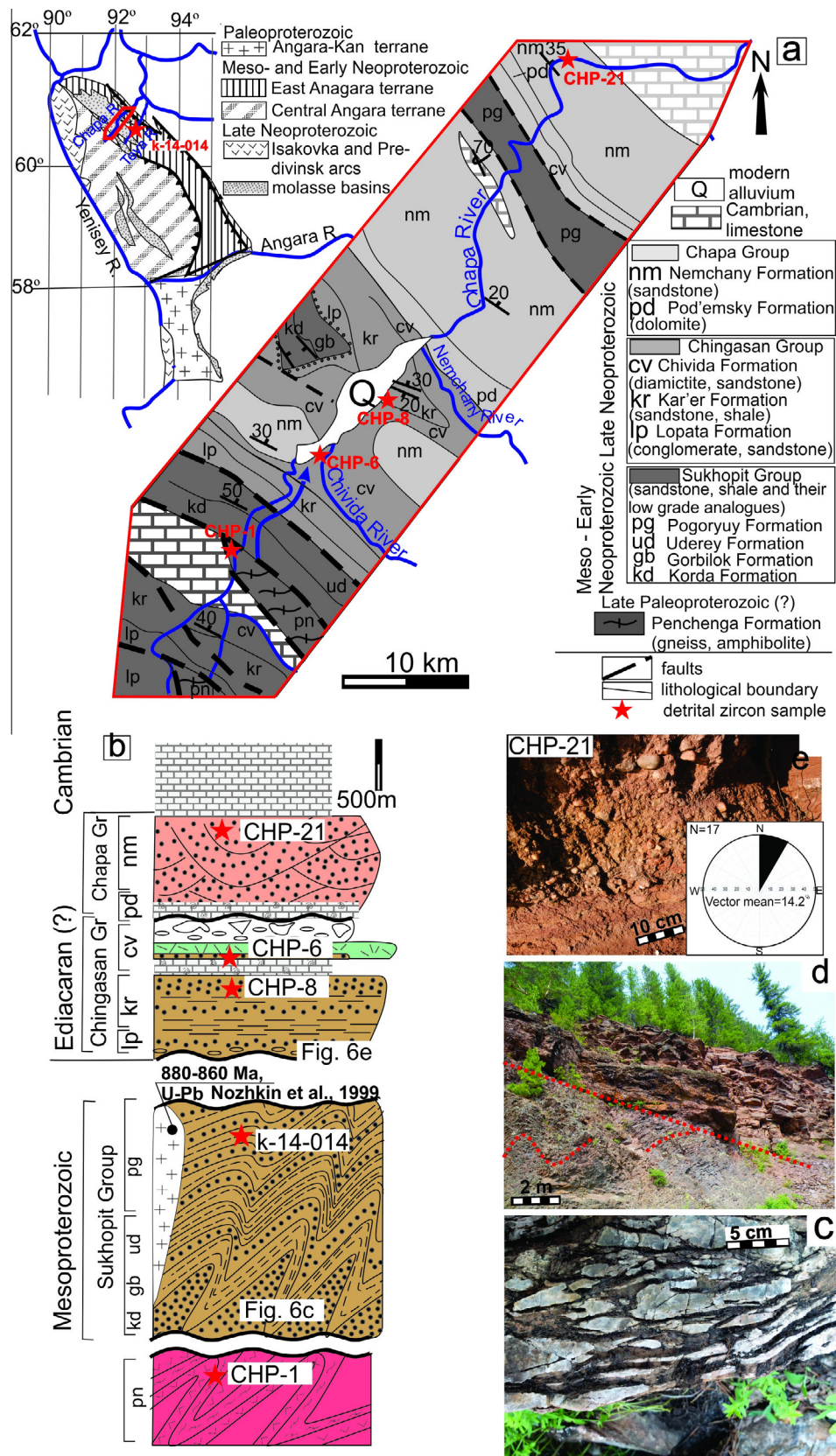


**Fig. 6.** Geology of the Teya-Chapa basin. Geological map of the Teya-Chapa basin (red frame, a) after Pokrovsky et al. (2012). Generalized stratigraphy of the Teya-Chapa basin and underlying metasedimentary units (b) compiled from Nozhkin et al. (2007), Vrublevich (1973), Karpinsky and Karpinskaya (1974); (c) shows isoclinally folded quartzite of Korda Formation exemplifying metasedimentary basement to Teya-Chapa basinal deposits; (d) shows unconformity between the Sukhopit and Chingasan groups; (e) shows red fluvial sandstone and embedded pebbles of Nemchan Formation, with cross bedding orientation (inset) indicating NNE direction of paleocurrents.



The Penchenga Formation, underlying the Sukhopit Group, is predominantly represented by graphite bearing quartz–biotite, biotite–amphibole, biotite–garnet schists alternating with marbles, and rare beds of quartzite (Nozhkin et al., 2012). The clastic succession incorporates the large Indyglinsky amphibolite suite and is interpreted as rift-related (Nozhkin et al., 1999, 2012).

The stratigraphy of the overlying Teya-Chapa basin (Fig. 6b), separated by an angular unconformity from the Sukhopit Group (Fig. 6d), has been described in detail by Nozhkin et al. (2007) and Pokrovsky et al. (2012). Within the study area, the basinal fill is gently folded and form two major sedimentary cycles, namely the Chingasan and the Chapa groups. The 2 km thick Chingasan Group is predominantly composed of a lowermost conglomerate, followed by shallow-marine successions of interbedded sandstone and calcareous siltstone. The uppermost Chivida Formation is remarkable because of its diamictite succession, attributed to the ~720 to 700 Ma Sturtian glaciation (Postel'nikov, 1981; Sovetov and Komlev, 2005). Near the Vorogovka River, the Chivida Formation also hosts  $703 \pm 4$  Ma old trachyte (Nozhkin et al., 2007), although it does not occur in the study region.

Chapa Group deposition commenced with dolostone and siltstone of the Pod'emny Formation but rapidly passed into red fluvial cross beds of the Nemchan Formation (Fig. 6e), with thickness estimates between 1200 m (Sovetov et al., 2007) and 3000 m (Nozhkin et al., 2007). The Ediacaran age was supported by chemostratigraphic from the Pod'emny dolostones (Pokrovsky et al., 2012; Sovetov et al., 2007). However, recently reported paleontological and paleomagnetic studies suggest an earliest Cambrian (Nemakit-Daldynian) age for the base of the Chingasan Group (Shatsillo et al., 2015; Kuznetsov et al., 2013), challenging the accepted regional stratigraphic correlation.

## 5.2. Sample descriptions and results of U–Pb dating

### 5.2.1. Penchenga Formation (CHP-1)

The sample CHP-1 was collected near the Chapa River (Fig. 6a, Attachment 1). The sample is a red paragneiss (meta-arkose) with an overall composition of ~50% quartz, ~20% K-feldspar, ~20% muscovite and 10% opaque components. The studied paragneiss is interbedded with quartz-sericite and amphibole schist. In the thin section the paragneiss displays a metamorphic fabric, with quartz and feldspar subgrains wrapped by an anastomosing foliation outlined by bands of aligned mica grains (Fig. 7a). The micaceous bands (30–40% of total area of thin section) consist of fine muscovite (50%) and dark brown opaque grains (50%). Accessory phases include sphene, minor zircon and apatite. The extracted zircon grains are represented mostly by euhedral 100–150  $\mu$ m long grains, of which >70% retain facets, and ~30% are subrounded. They are zoned commonly and frequently show core–rim relations (Fig. 8a).

Sample CHP-1 had analysis conducted on 105 detrital zircon grains, of which 94 meet 5% discordance criteria. The obtained detrital zircon ages have low variance and fall within narrow range from  $1743 \pm 22$  Ma to  $1855 \pm 23$  Ma, forming a single zircon population that defines the 1790 Ma peak (Fig. 9a). However, the mean age of the youngest cluster define MDA as  $1743 \pm 22$  Ma ( $n = 3$ , MSWD = 0.39) and the YSG age is  $1743 \pm 22$  Ma. Both the peak population and the maximum depositional age seem to be close to the assumed 1650 Ma age of sedimentation (Nozhkin et al., 2009; Nozhkin et al., 2012).

### 5.2.2. Pogor'uy formation (k-14-014)

The sample k-14-014 was collected in the bed of the Teya River (Attachment 1). The sandstones from the Pogor'uy Formation (Fig. 6b) are dominated by medium grained quartz arenite. The framework (100% of total thin section area) consists almost solely

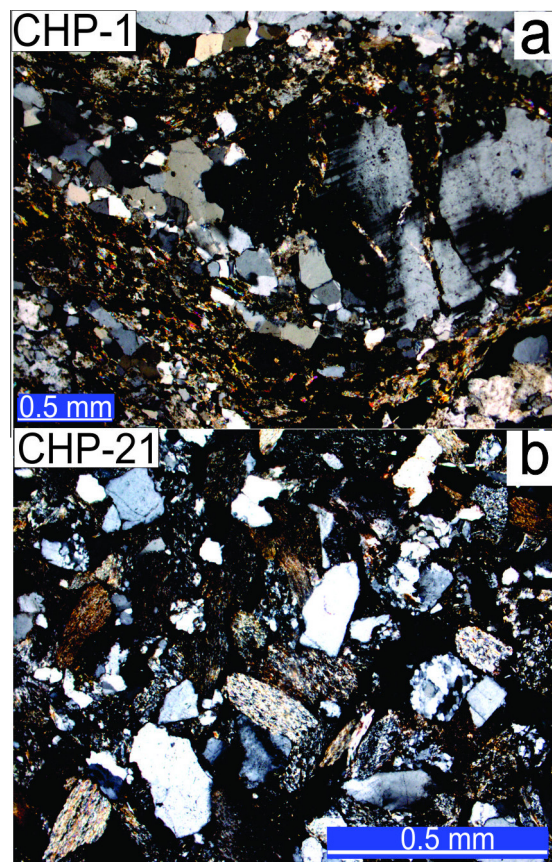


Fig. 7. Microphotographs of the representative thin-sections under cross polarized light; (a) paragneiss of the Penchenga Formation; (b) lithic arenite of the Nemchan Formation.

of well-sorted, subrounded, predominantly monocrystalline quartz grains that are 0.3–0.4 mm in diameter. Minor components (<5%) are K-feldspar and plagioclase. Zircon is present as an accessory mineral.

The extracted zircon grains are 100–150  $\mu$ m long, predominantly colourless. ~50% of the population are rounded grains while the other 50% are subrounded and retain prismatic shape.

The sample k-14-014 had 69 detrital zircon grains successfully analyzed, of which 62 meet the 5% discordance criteria. The detrital zircon ages in sample k-14-014 range from  $1596 \pm 53$  Ma to  $2986 \pm 30$  Ma (Fig. 9b). The predominant 2100–1800 Ma zircon population (60%) is commonly represented by subrounded prismatic grains. It defines major peak at ca. 1900 Ma and minor peak at ca. 2020 Ma. Another 40% of all concordant grains are mostly rounded and have ages in the range of 2450–3000 Ma. The most significant peak for this part of the age spectrum is 3000 Ma. MDA determined based on the mean age of the youngest cluster is  $1838 \pm 22$  Ma ( $n = 3$ , MSWD = 0.34), and based on YSG age is  $1596 \pm 53$  Ma.

### 5.2.3. Chingasan Group: Kar'er Formation (CHP-8)

Sample CHP-8 was collected on the Chapa River (Fig. 5a, b, d, Attachment 1). The yellowish, coarse grained, limonitized calcareous sublitharenite sandstone represents one of the sandstone packages within a sequence of interlayered yellowish sandstone and calcareous siltstone units. The framework (75% of total thin section area) consists of fine well sorted grains of subangular to rounded monocrystalline (85% of detrital grains) and polycrystalline quartz (10%), phyllite fragments (5%), rare feldspar represented by orthoclase (kaolinitized) and plagioclase. Nearly 40% of monocrystalline

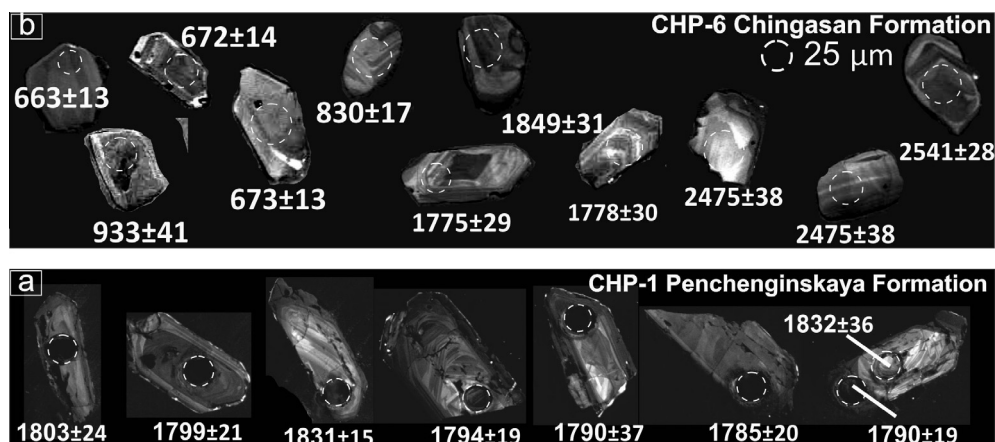


Fig. 8. Representative cathodoluminescence images of selected detrital zircon grains from samples CHP-1 (a) and CHP-6 (b).

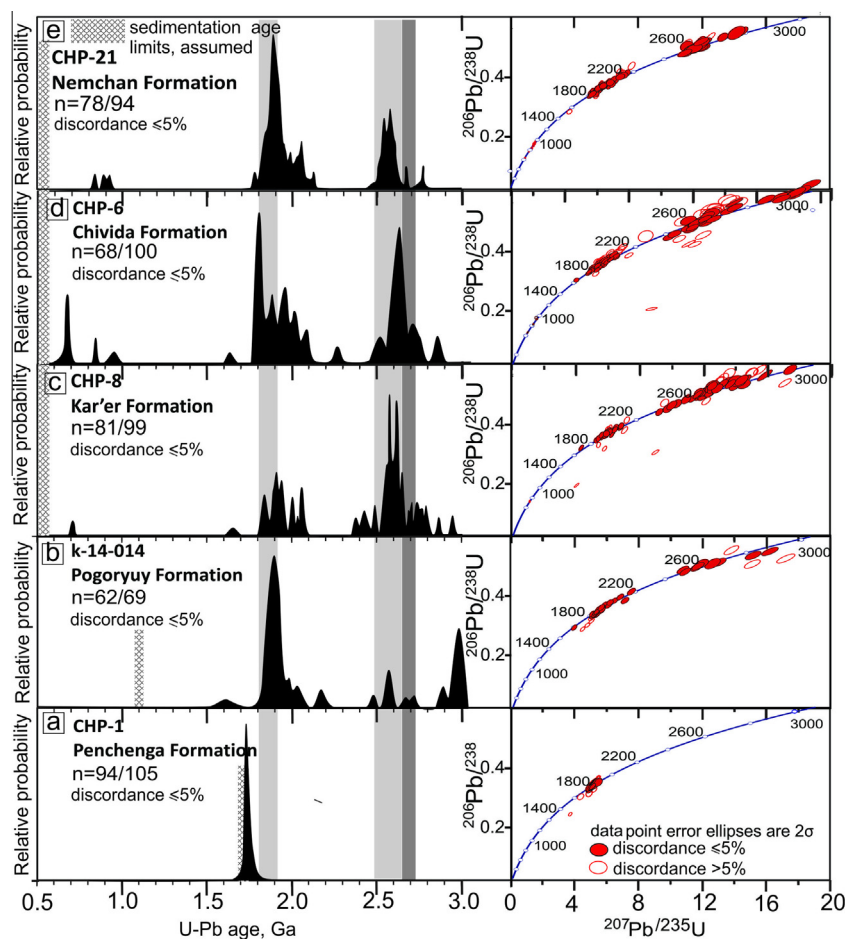


Fig. 9. Obtained age spectra with related concordia plots (right hand side) of detrital zircon populations for Penchenga Formation (a), Kar'er Formation (b), Chivida Formation (c), upper Nemchan (d). See explanations for sedimentation age limits in text.

quartz grains show undulose extinction. Cement (25%) consists of fine grained, locally recrystallized carbonate intergrown with a brown opaque aggregate. Titanite and zircon are accessory minerals.

The separated zircons are represented mostly by subrounded 50–100 µm long grains of which <30% retain prismatic shape and only few show facets. CHP-8 had 99 detrital zircon grains success-

fully analyzed, of which 81 meet 5% discordance criteria. The detrital zircon ages range from  $728 \pm 18$  Ma to  $2941 \pm 14$  Ma (Fig. 9c). A large population (61%) that falls between 2430 Ma and 2800 Ma defines a major probability density peak at 2590 Ma. Paleoproterozoic zircons (32%) form two populations, minor 2100–2000 Ma that defines a peak at 2070 Ma, and major 2000–1800 Ma that defines a strong peak at 1870 Ma. MDA based on mean age of the

youngest cluster is  $1847 \pm 16$  Ma ( $n = 3$ , MSWD = 0.064) and based on the YSG age the MDA is  $728 \pm 18$  Ma. The YSG age is close to the assumed age of deposition.

#### 5.2.4. Chingasan group: chivida formation (CHP-6)

Sample CHP-6 was collected near the junction of the Chapa and Chivida rivers (Fig. 6a and b). The sample is a grey medium-grained lithic arenite, with locally imbedded 1–5 cm mud chips and ripple mark surfaces. The framework (80% of total area of thin section) consists of well sorted grains of subrounded to rounded quartz (65% of detrital grains), shale fragments (15%) and detrital calcite/dolomite (20%). Quartz grains are predominantly monocrystalline (85%), with ~50% showing undulose extinction, and ~15% of quartz detritus is polycrystalline. Cement (20%) consists of fine grained, locally recrystallized carbonate. The accessory phases are opaque minerals, zircon and titanite.

The sample CHP-6 had 100 detrital zircon grains successfully analyzed, of which 68 meet the 5% discordance criteria. The detrital zircon ages in sample CHP-6 range from  $663 \pm 13$  Ma to  $2807 \pm 27$  Ma. The predominant 2100–1800 Ma zircon population (50%) is represented by prismatic grains, that frequently retain facets (Fig. 8b). It shows a triple peak at 1850 Ma, 1950 Ma, and 2020 Ma (Fig. 9d). Another major zircon population (40%, commonly rounded grains) has a peak at 2590 Ma and is represented by grains with ages between 2700 and 2430 Ma. MDA determined based on the mean age of the youngest cluster is  $670 \pm 8$  Ma ( $n = 3$ , MSWD = 0.72), and based on YSG age is  $663 \pm 13$  Ma. The youngest grains are subrounded, but frequently retain facets (Fig. 8b).

#### 5.2.5. Chapa group: Nemchan Formation (CHP-21)

Sample CHP-21 was collected from riverbank outcrop on the Chapa River and represents the upper part of the Nemchan Formation. It is a red sandstone classified as fine grained lithic arenite. The sandstone displays planar crossbedding that indicates consistent ENE direction of paleocurrent. The framework (>95% of total area of thin section) is poorly sorted, consists of subangular quartz grains (40%) and squashed lithic fragments (60%) that form pseudomatrix to the rock. 85% of quartz is monocrystalline but shows undulose extinction, and 15% of quartz is polycrystalline. Lithic fragments (Fig. 7b) are represented by phyllite (90%) and shale (10%). Cement comprises 10% of the rock and is represented by limonite aggregate that fills in the pore space. Accessory opaque phase is probably represented by magnetite partially altered to iron hydroxides aggregate.

The separated zircon population is represented by 30–100  $\mu$ m long, mostly rounded grains, though few grains preserve sharp facets. The sample CHP-21 had 94 successfully analyzed grains, of which 78 meet discordance criteria. The entire zircon population includes grains of Archean (31%), Paleoproterozoic (65%) and Neoproterozoic (4%) age (Fig. 9e). The 2150–1850 Ma zircon population forms minor peak near 2000 Ma and major peak near 1880 Ma. Archean grains are mostly 2600–2500 Ma old, defining a peak near 2580 Ma. Few grains fall in the age range of 2800–2600 Ma. MDA determined based on the YSG age is  $834 \pm 19$  Ma and is close to the assumed age of deposition, and the MDA based on mean value of youngest cluster is  $1834 \pm 14$  ( $n = 3$ , MSWD = 0.43).

## 6. East Anabar basin

### 6.1. Stratigraphy and sedimentary evolution

Meso- to Neoproterozoic rocks related to the East Anabar basin are exposed along the eastern slope of the Anabar Shield (Figs. 1 and 10). The basal deposits unconformably rest above the

Paleoproterozoic metagreywackes and calc-silicate rocks of the Hapchan Group and the NNW trending Billyakh melange zone that accommodates ca. 1.96–1.98 Ga granite intrusions (Smelov et al., 2012). Near its the western edge, the basin overlies high-grade metamorphic units of the Daldyn terrane, where age estimates range between 3.35 Ga and 2.76 Ga (Gusev et al., 2013; Rosen and Turkina, 2007, and Ref. therein). In the eastern part of the basin, the Meso- to Neoproterozoic succession thickens and is buried beneath the Paleozoic platform cover.

The studied stratigraphic section of the East Anabar basin comprises fluvial and shallow marine predominantly clastic sedimentary rocks. The studied rocks were recovered from drill cores and described in detail by Kuptsova et al. (2011) (Fig. 10, Attachment 1). In brief, the section consists of 5 main units (Fig. 10b) unconformably overlying the Billyakh melange zone (Fig. 10). Unit 1 (40–120 m thick) comprises several tens of meters thick sedimentary rhythmic cycles discontinued by erosional surfaces, typical of fluvial deposits. Each rhythm commences with conglomerate that contains abundant fragments of underlying metamorphic basement, passes upward into red cross-bedded sandstone and terminates with siltstone. By contrast, the sandstones of unit 2 display the horizontal bedding and contain glauconite, suggesting deposition in a shallow marine environment. Unit 2 (60–80 m) is made up of pinkish, poorly sorted cross-bedded sandstone with composition broadly similar to that of Unit 1. The sandstones of both units plot in quartz arenite and arkosic fields on the QFL diagram (Kuptsova et al., 2011). Unit 3 (90–150 m) is dominated by purple siltstone and shale, with interlayers of medium-grained quartz arenite. These are overlain by Unit 4 that comprises dolostones with interlayers of siltstone and grey subarkosic sandstone with abundant fragments of carbonate rocks. Unit 4 is topped by dolostone (Unit 5). The age of Proterozoic sedimentary units of the East Anabar basin has been debated. According to Kuptsova et al. (2015), Unit 1 is correlated with Mesoproterozoic Mukun Group, and units 4 and 5 with Ediacaran Staraya Rechka Formation, while units 2 and 3 were inferred to represent a previously unknown in the area Neoproterozoic unit. In most sections of both West and East Anabar basins, the Staraya Rechka Formation overlies older units with a clear erosional surface at the base, corresponding to the hiatus between two major sedimentary cycles on the platform.

### 6.2. Sample description and results of U-Pb dating

Lithological features of the studied samples have been described in detail by Kuptsova et al. (2011, 2015). In this paper, we briefly summarize petrographic descriptions of samples and present results of additional LA ICP-MS detrital zircon dating, combined with SHRIMP data previously obtained by Kuptsova et al. (2015).

Sample A4 (Unit 1) is red, medium- to coarse grained arkose (Fig. 11c) with relic cross bedding suggesting fluvial origin. The framework of sandstone consists of poorly sorted, angular to rounded grains of quartz (40–80% of detrital grains), feldspar (20–40%), and rounded fragments of quartzite, gneiss, and altered mafic rocks (10%). The sample also reveals a broad variety of accessory minerals. The recovered zircons are clear, rounded to subrounded ~100–300  $\mu$ m long grains, of which ~30% retain prismatic shape. The sample had 69 grains analysed using LA ICP-MS, that significantly complemented the previous SHRIMP study (Kuptsova et al., 2015) of 38 grains (Fig. 12a). Of 60 grains (this study) that meet the 5% discordance criteria, 80% are represented by 2200–1900 Ma zircon population that defines a prominent peak at 1970 Ma. The remaining 20% of grains have Archean ages in the range of 2950–2550 Ma. There is no obvious correlation between grain ages and degree of roundness. MDA (LA ICP MS and SHRIMP results combined), based on mean age of the youngest



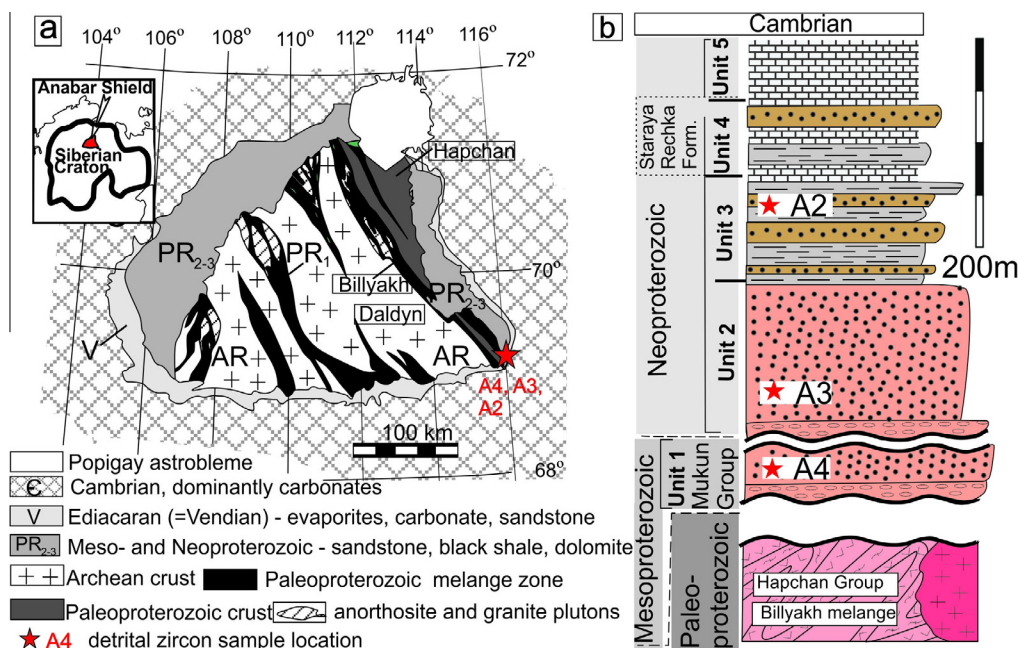


**Fig. 10.** Simplified geological map of the Anabar Shield area (a) after Molchanov et al. (2011) and stratigraphy of the southernmost East Anabar basin succession with detrital zircon sampling locations (a) after Kuptsova et al. (2015). The inset shows location of the Anabar Shield.

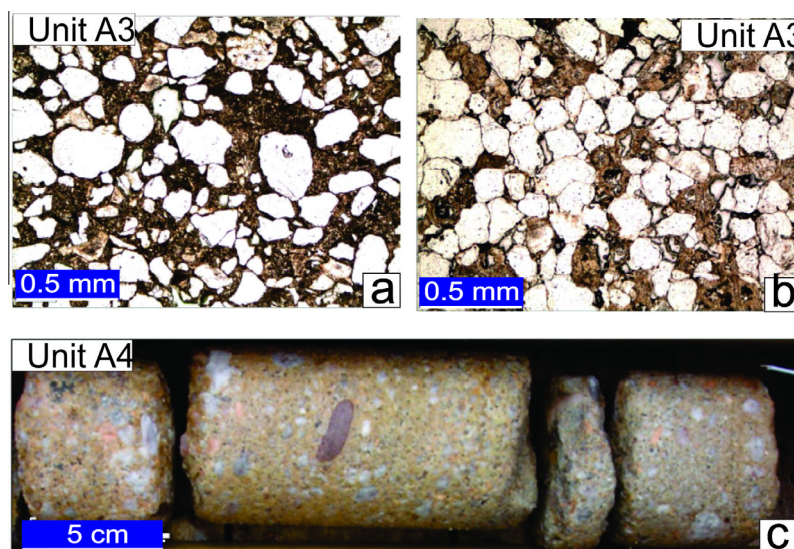


**Fig. 11.** Microphotographs (a and b) under plane light and photographs of representative samples (c) (Kuptsova, 2012) showing arkosic nature of unit 1 (sample A4) and replacement of feldspar by clayey materials. Note poorly sorted grains and presence of pink K-feldspar, lithic fragments in the sandstone from the unit 4 (c). For sedimentation age limits see explanations in text.

cluster, is  $1907 \pm 12$  Ma ( $n = 3$ , MSWD = 0.034) and based on YSG age is  $1914 \pm 19$  Ma. Both ages of the youngest cluster and YSG ages are at least  $\sim 200$  Ma older than the assumed age of the correlative Mukun Group.

Sample A3 (Unit 2) is a pinkish arkose sandstone (Fig. 11a and b) that preserves both horizontal and cross bedding. The framework is poorly sorted and consists of rounded quartz (90–50% of detrital grains), angular feldspar (10–40%) and lithic fragments (10%), cemented dominantly by illite (Fig. 11a and b). Laminae of well sorted quartz arenite are present. Feldspars are mostly microcline, but also plagioclase with composition of An70–80 is present. A wide range of accessory minerals occurs in the sample. The recovered zircons are clear rounded to subrounded

$\sim 700$ – $200$   $\mu$ m grains, of which  $\sim 50\%$  retain prismatic shape. The sample had 57 grains analysed by LA ICP-MS (this study) and 41 grains previously analysed by SHRIMP (Kuptsova et al., 2015). Of 57 grains successfully analysed by LA ICP-MS 34 grains meet the 5% discordance criteria, of which 53% have mid-late Paleoproterozoic ages, and the remaining grains are early Paleoproterozoic and Archean (Fig. 12b). The mid-late Paleoproterozoic part of the age spectrum is dominated by a 2060–1920 Ma zircon population with major peak at ca. 2040 Ma and minor peak at 1940 Ma. When plotted on concordia (Fig. 12b), a significant amount of data points is uniformly distributed along the spectrum between 2950 and 2100 Ma, defining a discordia with upper intercept at  $2957 \pm 40$  Ma and lower intercept at  $1935 \pm 25$  Ma. The MDA (LA

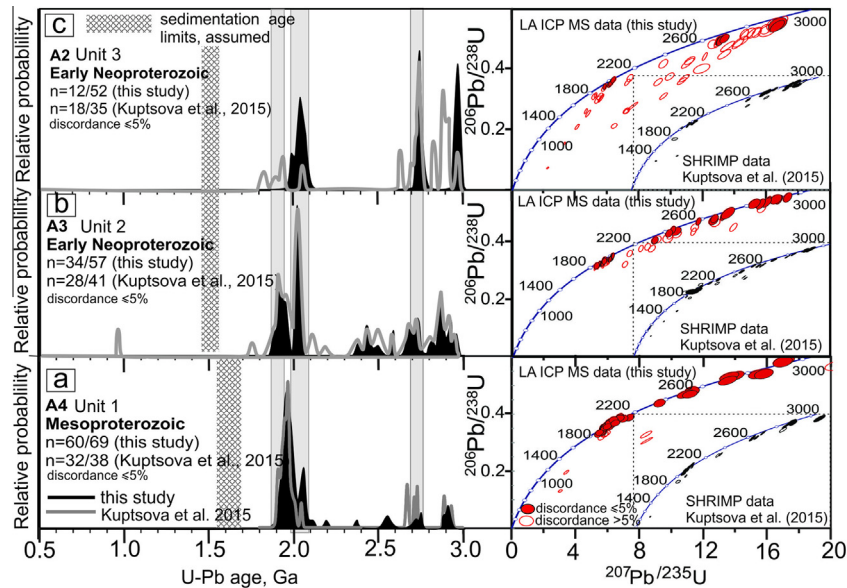


**Fig. 12.** Obtained age spectra (LA ICP-MS results of this study are compared with SHRIMP data of Kuptsova et al. (2015) and related concordia plots for detrital zircon populations from the east Anabar basinal deposits.

ICP MS and SHRIMP results combined) determined based on mean age of the youngest cluster is  $1892 \pm 16$  Ma ( $n = 3$ , MSWD = 1.19) whereas the YSG age is  $919 \pm 43$  Ma, almost 1000 Ma younger than the youngest cluster age. The youngest grain was dated in 4 spots, yielding an upper-intercept discordia age at  $1028 \pm 94$  Ma (Kuptsova et al., 2015).

Sample A2 is a pinkish subarkosic sandstone that forms one of the packages in the siltstone-dominated Unit 3 (Kuptsova et al., 2011). Kuptsova et al. (2015) report that framework is represented by quartz (93–55% of detrital grains), feldspar (40–7%), and rock fragments (<3%). Sandstones are poorly sorted with both angular and rounded fragments. Cementing aggregate consists of regenerated quartz, illite, muscovite, minor carbonate and ferruginous. Zircon recovered from sample A2 are clear, subrounded  $\sim 70$ – $100$   $\mu$ m long grains, commonly retaining prismatic shape. The sample had 67 grains analysed by LA ICP-MS (this study) and 31 grains by SHRIMP (Kuptsova et al., 2015). Of the 52 accurate LA ICP MS analysis, only results for 12 grains meet the 5% discordance criteria. The obtained ages cluster near 2.05 Ga, 1.7 Ga and 2.95 Ga (Fig. 12c). MDA (LA ICP MS and SHRIMP results combined) determined based on mean age of the youngest cluster is  $2033 \pm 13$  Ma ( $n = 3$ , MSWD = 1.15) and based on the YSG age is  $1819 \pm 28$  Ma. However, both of them are significantly older than the age of the Mukun Group and YSG age of sample A3.

## 7. Discussion

### 7.1. Evaluating maximum depositional ages of the sedimentary succession

For the studied sedimentary basins of the SC, existing constraints for the age of Proterozoic sedimentary units come mainly from extrabasinal stratigraphic correlations based on lithology, biostratigraphy of microphytolites and stromatolites and, more rarely, on U-Pb dating and chemostratigraphy of carbonates (e.g. Bartley et al., 2001; Khabarov and Varaksina, 2011; Melnikov et al., 2005; Ovchinnikova et al., 1995; Semikhatov and Serebryakov, 1983; Shenfil', 1991). With the first U-Pb detrital zircon studies, the stratigraphy and depositional age of Precambrian

strata on the in SC and adjacent areas has begun to be revised significantly (e.g. Ershova et al., 2015; Kuptsova et al., 2015).

In the Turukhansk basin, based on paleontological and chemostratigraphic grounds the sedimentation age of the analysed Bezymenskaya Formation is estimated at  $\sim 1050$  Ma, Sukhaya Tunguska Formation at  $\sim 1035$  Ma, and Derevninskaya and Burovaya formations at  $\sim 1000$ – $900$  Ma (Petrov, 2006; Gallet et al., 2000; Petrov and Semikhatov, 2009). However, only our YSG age of  $1060 \pm 29$  Ma obtained for the Burovaya Formation is close to the assumed age of sedimentation for these Mesoproterozoic units. The  $\sim 630$  Ma age of the two youngest grains obtained for the late Ediacaran/Early Cambrian basal conglomerate package of the Platonovskaya Formation is compatible with the inferred Ediacaran sedimentation age. However, the MDA based on mean age of the youngest cluster is 1700 Ma, and is much less compatible with the inferred sedimentation age.

For the Yenisei Ridge region, this detrital zircon study provides the first zircon-based age constraints on high-grade metasedimentary basement units. The YSG and cluster-based MDAs for the Penchenga Formation, which is basement to the Teya-Chapa basin, define a reliable maximum deposition age of  $\sim 1740$  Ma. The zircons are euhedral and seem to be derived from a single proximal source. This age is only 100 Ma older than the assumed MDA age of ca. 1650 Ma age by Nozhkin et al. (2009), based on 1680–1660 K-Ar age of a biotite from the schist (Volobuev et al., 1976). However, given this is clearly a metamorphic age, the 1740 Ma MDA age is considered to more closely approximate the age of sedimentation.

By contrast, cluster based MDAs of  $670 \pm 8$  Ma (YSG) and  $663 \pm 13$  Ma (for the Chingasan Group in the Teya-Chapa basin (sample CHP-6) are younger than the previous  $\sim 700$  Ma age estimates, based on regional geological correlations (e.g. Nozhkin et al., 2007; Vernikovskiy et al., 2003; Khomentovskiy, 2007). The MDAs agree better with the recent latest Ediacaran/Early Cambrian age estimate of the Chingasan Group based on fossil findings and the paleomagnetic record (Shatsillo et al., 2015; Kuznetsov et al., 2014). Cluster based MDAs 660–630 Ma of the Chingasan and Chapa groups resemble the MDA based on YSG of  $632 \pm 17$  Ma obtained for late Ediacaran/Early Cambrian Platonovskaya conglomerate, suggesting that all Ediacaran–Early Cambrian

successions likely form the base of the same post-unconformity sedimentary cycle.

In samples CHP-8, CHP-21 from the Teya-Chapa basin, youngest single grain age better resemble the assumed ca. 550 Ma age of sedimentation (Shatsillo et al., 2015) than the cluster-based MDAs of ca. 740 Ma and ca. 960 Ma.

Our detrital zircon study of the Proterozoic succession of the East Anabar basin complements that by Kuptsova et al. (2015). The cluster-based MDA ages for all successions are ~1900 Ma and are significantly older than the assumed sedimentation age. However, based on the YSG age of  $919 \pm 43$  Ma (Kuptsova et al., 2015), it is suggested that deposition of Unit 3 occurred during the latest Mesoproterozoic or early Neoproterozoic.

## 7.2. Implications for evolution of sedimentary basins and their tectonic setting

Sedimentological evolution of the Turukhansk, Teya-Chapa and East Anabar basins is recorded by lithological diversity of their fills and detrital zircon signatures. In the East Anabar basin, the detrital zircon patterns of units 1, 2 and 3 are characterised by cluster-based MDAs of ca. 1900 Ma, at least 200 Ma older than the assumed sedimentation age. Supported by a fluvial origin of the sandstones and their local provenance (Kuptsova et al., 2015), this is consistent with deposition in a localised intracratonic basin.

In both the Turukhansk and Teya-Chapa basins located along the western margin of the SC, Proterozoic siliclastic deposition occurred through two main sedimentary cycles that accumulated in distinct tectonic settings, divided by the Ediacaran angular unconformity. In the Turukhansk basin, pre-unconformity successions formed during the latest Mesoproterozoic–Early Neoproterozoic and include siliclastic shallow marine deposits. These units are represented by submature arkose and quartz arenite that locally show very mature composition, consistent with intermittent reworking of the sediments.

The large age gap (~1000 Ma) between the MDA and inferred sedimentation ages points out a lack of syndepositional magmatism in the Turukhansk basin during the Meso- early Neoproterozoic, and is typical of passive margin settings (Cawood et al., 2012). A similar interpretation was suggested by Pisarevsky and Natapov (2003) and Vernikovskiy et al. (2009), based on the gradual westward thickening of sedimentary units as well as carbonate-siliclastic composition of the succession (Petrov, 1993). This setting is compatible with paleomagnetic reconstructions suggesting the margin faced an open ocean at the end of the Mesoproterozoic (Metelkin et al., 2015; Pisarevsky et al., 2008), but is not compatible with reconstructions that place the Grenville orogen between the western margin of Siberia and North China Craton (Likhonov et al., 2014) or India (Evans, 2009) within a Rodinia supercontinent. If such a configuration existed, Mesoproterozoic deposits near Turukhansk would have been intracontinental in their origin, and would have been likely to receive Grenville-derived detritus.

In the Yenisei Ridge region, the studied pre-Ediacaran units are represented by the latest Paleoproterozoic Penchenga metasedimentary formation that also hosts the Idyglinskii mafic complex (Nozhkin et al., 2012), and the Pogor'uy Formation of the Sukhopit Group. Perfectly euhedral shape of zircons indicates that the protolith of the Penchenga feldspathic paragneiss was derived directly from underlying basement units. They are most likely associated with  $1776 \pm 8$  Ma mafic granulites (Turkina et al., 2012a) or  $1780 \pm 10$  Ma A-type Taraka granites (Bibikova et al., 1993) of the southerly located Kan Uplift, consistent with its setting along the rifted margin of the SC. Probably, the late Paleoproterozoic rifting proceeded to formation of a passive margin, recorded by the Sukhopit Group (Nozhkin et al., 2009; Pisarevsky and Natapov, 2003), a potential correlative of the Bezymenskaya Formation in

the Turukhansk region. Pogor'uy Formation of the Sukhopit shows large gap between its cluster-based MDA (ca. 1800 Ma) and assumed age of sedimentation (1100 Ma), consistent with this assumption.

Therefore, the pre-Ediacaran unconformity units in the Turukhansk, Yenisei and Anabar regions are broadly similar, and appears to all have formed in extensional, either intracratonic (Anabar basin), or passive margin-type setting (Turukhansk and Yenisei regions).

Above the basal Ediacaran unconformity, the late Ediacaran/Early Cambrian Platonovskaya Formation of the Turukhansk region has an YSG age of ca. 630 Ma, close to the age of sedimentation. However, scarcity of young grains and the significant difference of ~80 Ma between MDA and sedimentation age suggests that the formation was probably deposited in the setting distal to a convergent plate margin (Cawood et al., 2012). The commonly rounded shape of zircons is indicative of intense sedimentary reworking. In terms of age and setting, the Platonovskaya Formation is comparable to the rock units of the Teya-Chapa basin of the north Yenisei Ridge, where the common ca. 670 Ma MDAs for all units are probably >100 Ma older than the sedimentation age assumed based on fossil records, and where the Neoproterozoic zircon grains are minor (<10%).

The presence of Neoproterozoic zircon grains in the post-unconformity successions of the Turukhansk and Yenisei Ridge regions along the western margin of the SC distinguishes them from underlying units. These grains may represent distal Neoproterozoic arc material that accreted to the northern or western margin of the SC prior to or during formation of the Ediacaran angular unconformity (Pisarevsky and Natapov, 2003; Vernikovskiy et al., 2009, 2004). Although the dataset for the Chapa Group indicating NNE paleocurrent directions is too small to draw solid conclusions, it is remarkably consistent with NE directions measured by Sovetov et al. (2007), indicating transport from the Yenisei Ridge orogen to the platform. The generally immature composition of the sediments also suggests that some of euhedral Neoproterozoic zircons in the studied sedimentary rocks (Fig. 8b) could have been transported into the Teya-Chapa basin from the Neoproterozoic granitoids of the Yenisey Ridge. These include ca. 880–860 Ma Teya and Yeruda massifs, ca. 750–720 Ma Ayakhta and Glushikha granites, Predivinsk rhyolite ( $637 \pm 6$  Ma), Porozhnaya ( $697 \pm 4$  Ma) and Yagunov ( $628 \pm 3$  Ma) plagiogranite (Vernikovskiy et al., 2003, and Ref. therein).

Nonetheless, Neoproterozoic terranes served only as secondary sources for these rocks. Primarily, conglomerate of the Platonovskaya Formation and lithic arenites of the Chingasan and Chapa groups contain ca. 2.5–2.6 Ga and ca. 1.9–1.8 Ga material characteristic of the underlying pre-unconformity successions. Near Yenisei Ridge, the unique 1790 Ma peak of the late Paleoproterozoic Penchenga unit repeats above the unconformity in the Chivida Formation (compare Fig. 9a and d). The prominent 1.9 Ga peak of the detrital age spectrum of the pre-unconformity Pogor'uy Formation can be traced in the post-unconformity Nemchan Formation (compare Fig. 9b and e). One option is that both pre- and post-unconformity sediments received their detritus from proximal basement uplifts of the SC. Alternatively, in our preferred interpretation, the post-unconformity units could have formed through cannibalisation of the underlying metasedimentary basement and therefore both have similar detrital signatures. In the Yenisei Ridge area, lithic clasts from the pre-unconformity units constitute up to 50% of the framework in arenites of the post-unconformity Chingasan and Chapa groups. They are represented by phyllite and quartzite that can be directly related to the underlying Sukhopit Group. Similarly, the abundance of lithic fragments in the Platonovskaya conglomerate suggests that underlying deformed Meso- Neoproterozoic succession was eroded during



the late Neoproterozoic hiatus. Commonly rounded zircon grain shapes in all post-unconformity successions provide additional evidence for their recycled nature.

### 7.3. Detrital zircon signatures characterising the basement domains of the Siberian Craton

Lithological and sedimentological analysis of pre-unconformity sedimentary rocks from the Turukhansk and East Anabar basins indicates that the detritus mostly came from local uplifts of the cratonic interior. In the pre-unconformity sedimentary rocks from Turukhansk, both latest Neoproterozoic Archean and Paleoproterozoic zircon grains zircons often display prismatic and euhedral shapes. Further, the abundance of feldspar in immature sandstones of the Bezymenskaya Formation, along with abundant sulphides in glauconite sandstone from the Burovaya Formation, also indicate local provenance for the Turukhansk basin, although some sediments, such as the Derevninskaya mature quartz arenite, underwent some reworking. As pointed out by Kuptsova et al. (2015), the fluvial arkosic to subarkosic immature sandstones from the intracratonic East Anabar basin also provide direct information about underlying local crustal Archean and Paleoproterozoic units, partially exposed in the Anabar Shield. According to the contrasting detrital zircon age distributions between the East Anabar and Turukhansk-Yenisei Ridge regions (Fig. 14), the basins along the western margin of the SC were isolated from the East Anabar basin during the Meso- and early Neoproterozoic (Fig. 13a). Thus, U-Pb detrital zircon signatures from local sedimentary basins that existed in the western and northern parts of the SC during the Meso- and Neoproterozoic provide a tool to recognize the age of the buried cratonic basement.

Nearly all samples collected along the western margin of the SC from both the Turukhansk and Teya-Chapa basins reveal a major 2600–2450 Ma detrital zircon population, which defines a unique fingerprint for northwestern part of SC. The grains are often euhedral (Fig. 4b), supporting local provenance. The basins are underlain by Paleoproterozoic Angara belt and Archean Tungus block, which makes up almost the entire western half of the Craton (Fig. 13a). The Tungus block has its unique exposure in the south-westernmost part of the SC (Rosen et al., 1994), the Sharyzhgaly Uplift (Fig. 13a). A wide range of Paleoproterozoic and Neoproterozoic igneous and metamorphic suites with ages between ~3.4 and 2.5 Ga (Bibikova et al., 2006; Turkina et al., 2013, 2009, 2012b, 2014) has been reported from the uplift. Accordingly, 2.9–2.5 Ga detrital zircon signature is typical of numerous Neoproterozoic siliclastic units proximal to the Sharyzhgaly Uplift. These include the Baikal Group from southwesternmost part of the SC (Gladkochub et al., 2013), as well as Tertorga, Ballagannah, Dalne-taiga, Zhuya and Bodaibo Group from the Baikal-Muya belt, along the southern margin of the SC (Powerman et al., 2015). Possibly, rounded 3.0–2.5 Ga detrital zircons recovered from the Pogor'uy Formation in the north Yenisey Ridge region shared the same provenance with these units. In contrast to these units, detrital age spectra of the studied sedimentary rocks, except the Pogor'uy Formation, along the western part of the SC characterized by prominent 2.6–2.45 Ga peaks and minor abundance of the 2.9–2.7 Ga zircons (Figs. 5 and 9). The difference implies a heterochronous Tungus block, with its southern part potentially older than the buried northern section. The age transition in detrital age spectra of southern versus western parts of the SC can be directly related to Sharyzhgaly Uplift, where within the northern Kitoy domain numerous granite intrusions with ages between

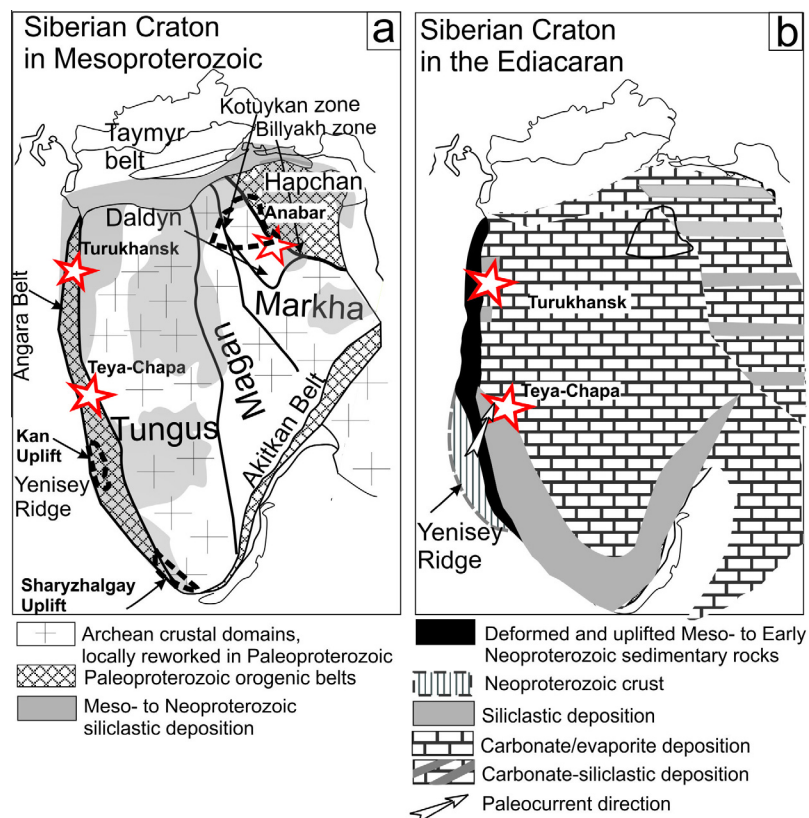


**Fig. 13.** Major crustal domains of the Siberian Craton and simplified paleogeography for Mesoproterozoic (a) and Ediacaran (b). On (a) Archean and Paleoproterozoic units after Rosen (2002) and Meso- to Neoproterozoic basins of siliclastic deposition after Frolov et al. (2015) and Khudoley et al. (2007). On (b) depositional environments based on data from Melnikov et al. (2005), Pelechaty (1998).

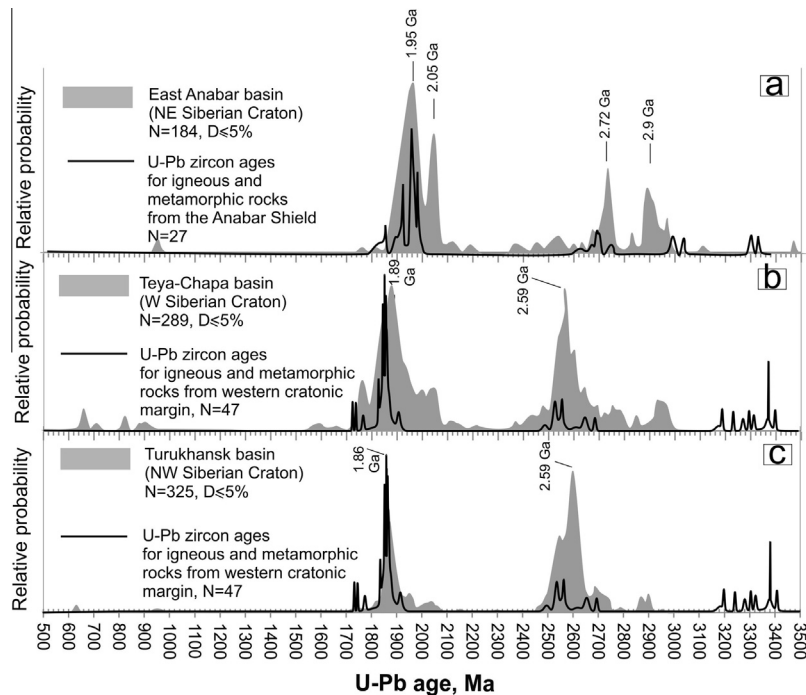


**Fig. 14.** Combined detrital zircon age spectra for the East Anabar (a), Teya-Chapa (b) and Turukhansk basins (c) compared with U-Pb ages of igneous rocks from local basement inliers. Source data and references are given in [Supplementary Table 2](#).

2625 and 2540 Ma intrude an older Nearchean basement (Gladkochub et al., 2009a; Turkina et al., 2012b; Sal'nikova et al., 2007). The granites and coeval high-grade metamorphic rocks (Poller et al., 2005; Turkina et al., 2012b) link the persistent detrital 2.6–2.45 Ga zircon population (Fig. 5 and 9) with Sharyzhalgay basement rocks. This leads us to consider that 2.6–2.45 Ga crust may constitute a significant part of the Tungus block, extending from the northernmost areas of the Sharyzhalgay Uplift to the northern margin of the Craton.

The Archean crust along the western margin of the SC is also significantly different from the crust recorded by sedimentary units of the East Anabar basin. The detrital zircon pattern of East Anabar basin comprises 2.9 Ga, 2.7 Ga and minor 2.6–2.45 Ga grains (Figs. 12 and 14a).

For all studied samples, Archean source rocks may include  $2702 \pm 9$  Ma Ust'-Monkhon monzodiorite (Gusev et al., 2013) and  $2760 \pm 10$  Ma (Bibikova et al., 1988) gneiss from the Daldyn complex. 2.7 Ga and locally 2.9 Ga crustal components are predominant Neoproterozoic constituents of the basement domains extending along the entire eastern part of the SC. The main Archean peak of 2.7 Ga has been recorded in detrital age spectra of most Meso- and Neoproterozoic sedimentary in the eastern part of the SC, including Mukun Group (Anabar Shield), Khaipakh and Uktinsk Formation (Kharaulakh Range) in the northeast, and Aimaghan, Kerpyl, Yudoma (Sette-Daban Range) in the southeast (Khudoley et al., 2015).

Other known Archean igneous suites in the Anabar Shield are dated at  $3320 \pm 100$  Ma,  $3000 \pm 20$  Ma (Bibikova et al., 1988),  $3050 \pm 12$  Ma,  $3012 \pm 15$  Ma (Gusev et al., 2013) and reasonably fit with the ca. 2950  $\pm$  40 Ma event identified by interpretation of detrital zircon data (Fig. 12). Therefore, the obtained detrital zircon data provide evidence for an extended distribution of previously underestimated 2.95 Ga crust near this part of the SC, or for a longer duration of the known ca. 3.0 Ga magmatic event.

Furthermore, two contrasting Paleoproterozoic signatures also characterise the crust in the western part of the SC and the eastern

Anabar Shield area. The composite detrital zircon spectra of the Turukhansk and Teya-Chapa basins (Fig. 14b and c) have strong 1.86 and 1.89 Ga peaks, respectively. The probable provenance of these zircon grains is widespread 1.84–1.87 Ga granitoids documented within the Sharyzhalgay Uplift and adjacent basement uplifts (Donskaya et al., 2014; Levitskii et al., 2002; Poller et al., 2005; Turkina et al., 2006), that may have formed a part of the Paleoproterozoic Angara orogenic belt (Rosen et al., 1994; Rosen and Turkina, 2007). In the immature sandstone of the Burovaya Formation the single population of euhedral zircons undoubtedly had a local source. The ca. 1.86 Ga age of this population suggests that the Angara belt extended as far north as the Turukhansk basin, as was predicted by Rosen et al. (1994) based on interpretations of magnetic field data. Additionally, the zircon populations with ages of 2100–1900 Ma and 1800–1750 Ma from the Teya-Chapa basin may correspond to early and late stages of magmatism in the Angara belt, respectively. The 2100–1900 Ma magmatic event has been previously inferred from detrital age spectra of the locally derived late Paleoproterozoic metasedimentary rocks of the Urik-Iya graben (Gladkochub et al., 2014). The 1800–1750 Ma zircon population may correspond to A-type granitic magmatism and granulite metamorphism that occurred near the western margin of the SC at 1840–1740 Ma (Turkina et al., 2012a, 2006; Bibikova et al., 1993). The 1.86 Ga prominent peak in the studied rock units is similar in age to the Paleoproterozoic peaks that fingerprint Neoproterozoic sedimentary rocks along the southern margin of the SC (Powerman et al., 2015; Gladkochub et al., 2013). These were deposited in the vicinity of the Akitkan, another Paleoproterozoic belt of the SC. However, little evidence exist to conclude about the provenance of these rocks. One option is that they were derived from the western margin of the SC, i.e., the Angara belt. Alternatively, the Angara and the Akitkan belts reveal similar detrital zircon fingerprints because they evolved contemporaneously.

By contrast, immature locally-derived sandstones of the East Anabar basin (Kuptsova et al., 2015 and this study), as well as sandstones from the northern margin of the Anabar Shield

(Khudoley et al., 2015), reveal older peaks of 1.95 Ga and 2.05 Ga in the detrital age spectra, suggesting that the Paleoproterozoic orogenic event took place significantly earlier in this part of the Craton than along its western margin. The 1.95 Ga peak can be linked with I-type granitic suites that occurred within the Billyakh melange zone (Fig. 10), including numerous quartz monzodiorites dated at  $1971 \pm 4$ ,  $1983 \pm 3$  Ma (Smelov et al., 2012),  $1985 \pm 13$  and  $1985 \pm 24$  (Molchanov et al., 2011). The range of  $\varepsilon_{\text{Nd}}$  (T) values for these granites extends from +1.6 to –8.9 (Molchanov et al., 2011; Smelov et al., 2012), suggesting they formed through mixing between juvenile Paleoproterozoic and Neoarchean components in a supra-subduction setting.

The major 2.15–2.0 Ga zircon population traced in the samples from East Anabar basin requires an earlier orogenic stage that predated emplacement of the ca. 1.95 Ga Billyakh granites. Igneous suites of comparable age have not yet been reported from the Anabar Shield, but may be located eastwards of the Billyakh melange zone and constitute part of the buried Hapchan terrane (Fig. 14), commonly referred to as Paleoproterozoic (Rosen, 2002; Glebovitsky et al., 2008) but never investigated directly. Remarkably, 2.15–1.95 Ga detrital signature characterises also some locally derived sedimentary rocks (e.g. Uchur Group) in the south-eastern margin of the SC (Khudoley et al., 2001, 2015), suggesting the distinct signal is typical of the SC in its eastern part. Further U–Pb–Hf detrital zircon studies from Proterozoic igneous and locally-derived sedimentary rocks will provide more information about the age and structure of heterogeneous Early Precambrian crust of the SC.

## 8. Conclusions

The following conclusions can be drawn:

- (1) Independent sedimentary basins existed on the Siberian Craton during the Meso- to Neoproterozoic, and they generally had local provenance. Near the eastern part of the Anabar Shield, the main suppliers of detritus were 2.9 Ga and 2.7 Ga, 2.15–2.0 and 2.0–1.9 Ga suites, such as Daldyn orthogneisses and Billyakh granitoids. Data from basins of the western SC margin suggest that early Paleoproterozoic–Archean crust in the northern part of Tungus block is dominated by 2.6–2.45 Ga suites, and the main Paleoproterozoic orogenic phase occurred at ca. 1.85–1.89 Ga, significantly later than in the eastern part of the Anabar Shield.
- (2) The late Paleoproterozoic, Mesoproterozoic and earliest Neoproterozoic sedimentary units of the Turukhansk basin and metasedimentary basement of the Teya-Chapa basin along the western margin of the Siberian Craton received detritus from proximal basement uplifts. Several lines of evidence, including the ca. 800 Ma gap between maximum depositional ages and the age of sedimentation in the Turukhansk area, suggest an intracratonic rift or passive margin setting for these basins.
- (3) The latest Ediacaran to Early Cambrian sediments along the western margin of the SC formed through recycling of deformed late Paleoproterozoic, Mesoproterozoic and earliest Neoproterozoic underlying sedimentary units. Contributions from Neoproterozoic detritus derived from arc terranes of the Yenisey Ridge are minor.

## Acknowledgements

N. Priyatkin supported by a University of Newcastle PhD scholarship, the project by an Australian Research Council grant

(DP120104004) and RFBF grant 15-35-20591. Study of A. Khudoley was supported by St. Petersburg State University research grant# 3.38.137.2014. W.J. Collins supported by an Australian Research Council grant (DP120104004). Study of N. Kuznetsov was supported by the Ministry of Science and Education of the Russian Federation (contract 14.Z50.31.0017 and grant 2330). This is contribution to the IGCP 648.

Comments made by Dr Randall Parrish (the Editor), an anonymous reviewer and Victor P. Kovach greatly improved the manuscript. NP also thanks P. Yu Petrov for his guidance during field work in the Turukhansk area, A.V. Shatsillo and O.M. Turkina for fruitful discussions on Precambrian geology of Siberia, Dr Angelos Maravelis for help processing paleocurrent data.

## Appendix A. Supplementary data

Supplementary data associated with this article can be found, in the online version, at <http://dx.doi.org/10.1016/j.precamres.2016.09.003>.

## References

- Bartley, J.K., Pope, M., Knoll, A.H., Semikhatov, M.A., Petrov, P.Y., 1998. A Vendian–Cambrian boundary succession from the northwestern margin of the Siberian Platform: stratigraphy, palaeontology, chemostratigraphy and correlation. *Geol. Mag.* 135, 473–494.
- Bartley, J.K., Semikhatov, M.A., Kaufman, A.J., Knoll, A.H., Pope, M.C., Jacobsen, S.B., 2001. Global events across the Mesoproterozoic–Neoproterozoic boundary: C and Sr isotopic evidence from Siberia. *Precamb. Res.* 111, 165–202.
- Bazanov, E.A., Pritula, Y.A., Zabaluev, V.V., 1976. Development of main structures of the Siberian platform: history and dynamics. *Tectonophysics* 36, 289–300.
- Bibikova, E.V., Belov, A.N., Rosen, O.M., 1988. Metamorphic rocks isotope dating in the Anabar shield. In: Markov, M.S. (Ed.), *Archean of the Anabar Shield and Problems of the Early Earth's Evolution*. Nauka, Moscow, pp. 122–133 (in Russian).
- Bibikova, E.V., Gracheva, T.V., Makarov, V.A., Nozhkin, A.D., 1993. The epochs of the Early Precambrian geologic evolution of the Yenisei Range, *Stratigrafiya. Geologicheskaya Korrelyatsiya* 1, 35–41 (in Russian).
- Bibikova, E.V., Turkina, O.M., Kirnozova, T.I., Fugzan, M.M., 2006. Ancient plagiogneisses of the Onot block of the Sharyzhgalskiy metamorphic massif: isotopic geochronology. *Geochem. Int.* 44, 310–315.
- Black, L., Gulson, B., 1978. The age of the mud tank carbonatite, Strangways range, Northern Territory. *BMR J. Aust. Geol. Geophys.* 3, 227–232.
- Cawood, P.A., Hawkesworth, C.J., Dhuime, B., 2012. Detrital zircon record and tectonic setting. *Geology* 40, 875–878.
- Cherepanova, Y., Artemieva, I.M., Thybo, H., Chemia, Z., 2013. Crustal structure of the Siberian craton and the West Siberian basin: an appraisal of existing seismic data. *Tectonophysics* 609, 154–183.
- Dickinson, W.R., Gehrels, G.E., 2009. Use of U–Pb ages of detrital zircons to infer maximum depositional ages of strata: a test against a Colorado Plateau Mesozoic database. *Earth Planet. Sci. Lett.* 288, 115–125.
- Donskaya, T.V., Gladkochub, D.P., Mazukabzov, A.M., Wingate, M.T.D., 2014. Early Proterozoic postcollisional granitoids of the Biryusa block of the Siberian craton. *Russ. Geol. Geophys.* 55, 812–823.
- Ernst, R., Buchan, K., Hamilton, M., Okrugin, A., Tomshin, M., 2000. Integrated paleomagnetism and u–pb geochronology of mafic dikes of the eastern anabar shield region, siberia: implications for mesoproterozoic paleolatitude of siberia and comparison with laurentia. *J. Geol.* 108, 381–401.
- Ershova, V.B., Prokopyev, A.V., Khudoley, A.K., Shneider, G.V., Andersen, T., Kullerud, K., Makar'ev, A.A., Maslov, A.V., Kolchanov, D.A., 2015. Results of U–Pb (LA–ICPMS) dating of detrital zircons from metaterrigenous rocks of the basement of the North Kara basin. *Dokl. Earth Sci.* 464, 997–1000.
- Evans, D.A.D., 2009. The palaeomagnetically viable, long-lived and all-inclusive Rodinia supercontinent reconstruction. Geological Society, London, Special Publications 327, 371–404.
- Frolov, S.V., Akhmanov, G.G., Bakay, E.A., Lubnina, N.V., Korobova, N.I., Karnyushina, E.E., Kozlova, E.V., 2015. Meso–Neoproterozoic petroleum systems of the Eastern Siberian sedimentary basins. *Precamb. Res.* 259, 95–113.
- Gallet, Y., Pavlov, V.E., Semikhatov, M.A., Petrov, P.Y., 2000. Late Mesoproterozoic magnetostratigraphic results from Siberia: paleogeographic implications and magnetic field behavior. *J. Geophys. Res. Solid Earth* 105, 16481–16499.
- Gehrels, G.E., 2009. Age Pick program, University of Arizona Laserchron Center.
- Gladkochub, D.P., Stanevich, A.M., Travin, A.V., Mazukabzov, A.M., Konstantinov, K. M., Yudin, D.S., Kornilova, T.A., 2009a. The Mesoproterozoic Udzha paleorift (Northern Siberian Craton): new data on age of basites, stratigraphy, and microphytology. *Dokl. Earth Sci.* 425, 371–377.
- Gladkochub, D.P., Donskaya, T.V., Reddy, S.M., Poller, U., Bayanova, T.B., Mazukabzov, A.M., Dril, S., Todt, W., Pisarevsky, S., Gladkochub, D.P., Donskaya, T.V., Reddy, S.M., Poller, U., Bayanova, T.B., Mazukabzov, A.M., Dril,



- S., Todt, W., Pisarevsky, S., 2009a. Palaeoproterozoic to Eoarchean crustal growth in southern Siberia: a Nd-isotope synthesis. In: Reddy, S. M., Mazumder, R., Evans, D. A. D., Collins, A. S. (eds.), *Palaeoproterozoic Supercontinents and Global Evolution*. The Geological Society of London, vol. 323, Special Publication, pp. 127–143.
- Gladkochub, D.P., Stanevich, A.M., Mazukabzov, A.M., Donskaya, T.V., Pisarevsky, S. A., Nicoll, G., Motova, Z.L., Kornilova, T.A., 2013. Early evolution of the Paleasian ocean: LA-ICP-MS dating of detrital zircon from Late Precambrian sequences of the southern margin of the Siberian craton. *Russ. Geol. Geophys.* 54, 1150–1163.
- Gladkochub, D.P., Mazukabzov, A.M., Stanevich, A.M., Donskaya, T.V., Motova, Z.L., Vanin, V.A., 2014. Precambrian sedimentation in the Uruk-lya Graben, southern Siberian Craton: main stages and tectonic settings. *Geotecton* 48, 359–370.
- Glebovitsky, V.A., Khil'tova, V.Y., Kozakov, I.K., 2008. Tectonics of the Siberian Craton: Interpretation of geological, geophysical, geochronological, and isotopic geochemical data. *Geotecton* 42, 8–20.
- Gusev, N.I., Rusenko, V.E., Berezhnaya, N.G., Skublov, S.G., Larionov, A.N., 2013. Isotope-geochemical features and age (SHRIMP) of metamorphic and magmatic rocks from the Kotuykan-Monkholinskaya zone of the Anabar Shield. *Reg. Geol. Metallogeny* 54, 45–59 (in Russian).
- Jackson, S.E., Pearson, N.J., Griffin, W.L., Belousova, E.A., 2004. The application of laser ablation-inductively coupled plasma-mass spectrometry to in situ U-Pb zircon geochronology. *Chem. Geol.* 211 (1–2), 47–69.
- Karpinsky, R.B., Karpinskaya, N.I., 1974. Geological map of USSR, sheet P-46-XXVII, Yenisey series, scale 1: 200,000. Aerogeological map, Moscow (in Russian).
- Khabarov, E.M., Varakina, I.V., 2011. The structure and depositional environments of Mesoproterozoic petroliferous carbonate complexes in the western Siberian craton. *Russ. Geol. Geophys.* 52, 923–944.
- Khomentovsky, V.V., 2007. The upper riphean of the Yenisei range. *Russ. Geol. Geophys.* 48, 711–720.
- Khudoley, A.K., Rainbird, R.H., Stern, R.A., Kropachev, A.P., Heaman, L.M., Zanin, A. M., Podkovyrov, V.N., Belova, V.N., Sukhorukov, V.I., 2001. Sedimentary evolution of the Riphean-Vendian basin of southeastern Siberia. *Precamb. Res.* 111, 129–163.
- Khudoley, A.K., Kropachev, A.P., Tkachenko, V.I., Rublev, A.G., Sergeev, S.A., Matukov, D.I., Lyahnitskaya, O.Y., 2007. Mesoproterozoic to Neoproterozoic evolution of the Siberian craton and adjacent microcontinents: An overview with constraints for a Laurentian connection. In: Link, P.K., Reed, S.L. (Eds.), *Proterozoic Geology of Western North America and Siberia*, vol. 86, SEPM Special Publication, pp. 209–226.
- Khudoley, A., Chamberlain, K., Ershova, V., Sears, J., Prokopyev, A., MacLean, J., Kazakova, G., Malyshev, S., Molchanov, A., Kullerud, K., Toro, J., Miller, E., Veselovskiy, R., Li, A., Chipley, D., 2015. Proterozoic supercontinental restorations: constraints from provenance studies of Mesoproterozoic to Cambrian clastic rocks, eastern Siberian Craton. *Precamb. Res.* 259, 78–94.
- Kotov, A.B., Sal'nikova, E.B., Glebovitsky, V.A., Kovach, V.P., Larin, A.M., Velikoslavinsky, S.D., Zagornaya, N.Y., 2006. Sm-Nd isotopic provinces of the Aldan Shield. *Dokl. Earth Sci.* 410, 1066–1069.
- Kovach, V.P., Kotov, A.B., Smelov, A.P., Starosel'tsev, K.V., Sal'nikova, E.B., Zagornaya, N.Y., Safronov, A.F., Pavlushin, A.D., 2000. Evolutionary stages of the continental crust in the buried basement of the eastern Siberian platform: Sm-Nd isotopic data. *Petrology* 8, 353–365 (in Russian).
- Kuptsova, A. V., 2012. Structure and evolution of uranium-bearing sedimentary basins exemplified by Pasha-Ladoga, East Anabar and Atabaska. Unpublished Cand. Sc. Thesis, 160p. (in Russian).
- Kuptsova, A.V., Khudoley, A.K., Molchanov, A.V., 2011. Lithogeochemistry of Meso- and Neoproterozoic terrigenous rocks of the southeast Anabar Basin: evolution of the composition of source rocks and epigenetic alterations. *Vestnik. St. Petersburg. Univ.*, Ser. 7 (1), 17–31 (in Russian).
- Kuptsova, A.V., Khudoley, A.K., Davis, W., Rainbird, R.H., Molchanov, A.V., 2015. Results of the U-Pb age of detrital zircons from Upper Proterozoic deposits of the eastern slope of the Anabar uplift. *Stratigr. Geol. Correl.* 23, 246–261.
- Kuznetsov, N.B., Shatsillo, A.V., Pavlov, V.E., Priyatkina, N.S., Danilko, N.K., Kozyonov, A.E., 2013. First findings of ichnofossils and arambriamorph structures in the rocks of the Chingasan and the Chapa Group of the Teya-Chapa basin (northeastern Yenisey Ridge). In: Sklyarov, E.V. (Ed.), *Proceedings of Meeting Geodynamic evolution of the Central Asian Orogenic Belt lithosphere (from ocean to continent)*, vol. 11. IZK SO RAN, Irkutsk, pp. 143–147 (in Russian).
- Letnikov, E.F., Kuznetsov, A.B., Vishnevskaya, I.A., Veshcheva, S.V., Proshenko, A.I., Geng, H., 2013. The Vendian passive continental margin in the southern Siberian Craton: geochemical and isotopic (Sr, Sm–Nd) evidence and U-Pb dating of detrital zircons by the LA-ICP-MS method. *Russ. Geol. Geophys.* 54, 1177–1194.
- Levitskii, V.I., Mel'nikov, A.I., Reznitskii, L.Z., Bibikova, E.V., Kirnozova, T.I., Kozakov, I.K., Makarov, V.A., Plotkina, Y.V., 2002. Early Proterozoic postcollisional granitoids in southwestern Siberian craton. *Geol. Geofiz.* 43, 717–731 (in Russian).
- Likhanov, I.I., Reverdatto, V.V., Vershinin, A.E., 2008. Fe- and Al-rich metapelites of the Teiskaya Group, Yenisei Range: geochemistry, protoliths, and the behavior of their material during metamorphism. *Geochim. Int.* 46, 17–36.
- Likhanov, I.I., Nozhkin, A.D., Reverdatto, V.V., Kozlov, P.S., 2014. Grenville tectonic events and evolution of the Yenisei Ridge at the western margin of the Siberian Craton. *Geotecton* 48, 371–389.
- Ludwig, K. R., 2003. *Isoplot: Berkeley Geochronology Center Special Publication No. 4*, 72p.
- Melnikov, N.V., Yakshin, M.S., Shishkin, B.B., Efimov, A.O., Karlova, G.A., Kilkina, L.I., Konstantinova, L.N., Kochnev, B.B., Kraevskiy, B.G., Melnikov, P.N., Nagovitsin, K. E., Postnikov, A.A., Ryabkova, L.V., Terleev, A.A., Khabarov, E.M., 2005. Stratigraphy of oil and gas basins of Siberia. Riphean and Vendian of Siberian platform and its plaited border. *Geo Novosibirsk* 428p. (in Russian).
- Metelkin, D.V., Vernikovskiy, V.A., Matushkin, N.Y., 2015. Arctida between Rodinia and Pangea. *Precamb. Res.* 259, 114–129.
- Molchanov, A.V., Knyazev, V.Yu., Khudoley, A.K., 2011. Tectonic-fluidothermal zones of the Anabar Shield and their ore potential. *Reg. Geol. Metallogeny* 47, 96–105 (in Russian).
- Nikishin, A.M., Sobornov, K.O., Prokopyev, A.V., Frolov, S.V., 2010. Tectonic evolution of the Siberian Platform during the Vendian and Phanerozoic. *Moscow Univ. Geol. Bull.* 65, 1–16.
- Nozhkin, A.D., Nozhkin, A.D., Turkina, O.M., Bibikova, E.V., Terleev, A.A., Khomentovsky, V.V., 1999. Riphean granite gneiss domes of the Yenisei Range: geological structure and U-Pb isotopic age. *Geol. Geofiz. (Russian Geology and Geophysics)* 40 (9), 1305–1313 (in Russian).
- Nozhkin, A.D., Postnikov, A.A., Nagovitsin, K.E., Travin, A.V., Stanevich, A.M., Yudin, D.S., 2007. Neoproterozoic Chingasan Group in the Yenisei Ridge: new data on age and deposition environments. *Russ. Geol. Geophys.* 48, 1015–1025.
- Nozhkin, A.D., Turkina, O.M., Maslov, A.V., Dmitrieva, N.V., Kovach, V.P., Ronkin, Y.L., 2009. Sm–Nd isotopic systematics of Precambrian carbonates from the Yenisei range and age variations of their provenances. *Dokl. Earth Sci.* 423, 1495–1500.
- Nozhkin, A.D., Dmitrieva, N.V., Turkina, O.M., Maslov, A.V., Ronkin, Y.L., 2010. Lower precambrian metapelites of the Yenisei Range: REE systematics, provenances, paleogeodynamics. *Dokl. Earth Sci.* 434, 1390–1395.
- Nozhkin, A.D., Maslov, A.V., Dmitrieva, N.V., Ronkin, Y.L., 2012. Pre-Riphean metapelites of the Yenisei Range: chemical composition, sources of eroded material, and paleogeodynamics. *Geochem. Int.* 50, 574–610.
- Ovchinnikova, G.V., Semikhatov, M.A., Gorokhov, I.M., Belyatskii, B.V., Vasilieva, I.M., Levskii, L.K., 1995. U-Pb systematics of Pre-Cambrian carbonates: the riphean sukhaya tunguska formation in the Turukhansk Uplift, Siberia. *Lithol. Min. Resour.* 30, 477–487.
- Paton, C., Woodhead, J.D., Hellstrom, J.C., Hergt, J.M., Greig, A., Maas, R., 2010. Improved laser ablation U-Pb zircon geochronology through robust downhole fractionation correction. *Geochim. Geophys. Geosyst.* 11 (3).
- Pelechaty, S.M., 1998. Integrated chronostratigraphy of the Vendian System of Siberia: implications for a global stratigraphy. *J. Geol. Soc.* 155, 957–973.
- Petrov, P.Yu., 1993. Structure and depositional environments of the Riphean Bezymenskaya formation in the Turukhansk Uplift, Siberia. *Stratigr. Geol. Correl.* 1 (5), 20–32 (in Russian).
- Petrov, P.Y., 2000. The clayey-carbonate sedimentation cycle and carbonate platform formation: evidence from the linok formation, the middle riphean of the turukhansk uplift, siberia. *Lithol. Min. Resour.* 35, 232–251.
- Petrov, P.Y., 2001. Microbial mats as a source of carbonate sediments in the late precambrian: evidence from the linok formation, the middle riphean of the Turukhansk Uplift, Siberia. *Lithol. Min. Resour.* 36, 164–186.
- Petrov, P. Yu., 2006. Riphean basins of the Turukhansk Uplift of Siberia: origin, geological history and importance of biological component in sedimentary processes. Unpublished Cand. Sc. Thesis summary, p. 25. (in Russian).
- Petrov, P.Y., 2011. Molar tooth structures: formation and specificity of carbonate diagenesis in the Late Precambrian, Middle Riphean Sukhaya Tunguska Formation of the Turukhansk Uplift, Siberia. *Stratigr. Geol. Correl.* 19, 247–267.
- Petrov, P.Y., Semikhatov, M.A., 2001. Sequence organization and growth patterns of late Mesoproterozoic stromatolite reefs: an example from the Burovaya Formation, Turukhansk Uplift, Siberia. *Precamb. Res.* 111, 257–281.
- Petrov, P.Y., Semikhatov, M.A., 2009. Platforms: shorikha formation of the Turukhansk uplift, Siberia. *Stratigr. Geol. Correl.* 17, 461–475.
- Pisarevsky, S.A., Natapov, L.M., 2003. Siberia and rodinia. *Tectonophysics* 375, 221–245.
- Pisarevsky, S., Natapov, L.M., Donskaya, T.V., Gladkochub, D.P., Vernikovskiy, V.A., 2008. Proterozoic Siberia: a promontory of Rodinia. *Precamb. Res.* 160, 66–76.
- Pokrovsky, B.G., Bujakaite, M.I., Kokin, O.V., 2012. Geochemistry of C, O, and Sr isotopes and chemostratigraphy of neoproterozoic rocks in the northern Yenisei Ridge. *Lithol. Min. Resour.* 47, 177–199.
- Poller, U., Gladkochub, D., Donskaya, T., Mazukabzov, A., Sklyarov, E., Todt, W., 2005. Multistage magmatic and metamorphic evolution in the Southern Siberian Craton: archaic and Palaeoproterozoic zircon ages revealed by SHRIMP and TIMS. *Precamb. Res.* 136, 353–368.
- Postel'nikov, E.S., 1981. Late Precambrian Chivida Tilloids of the Yenisei Ridge and Central Siberia. U.S.S.R. In: Hambrey, M.J., Harland, W.B., (Eds.), *Earth's Pre-Pleistocene Glacial Record*, Cambridge, Cambridge Univ. Press, pp. 375–379.
- Postel'nikov, E.S., 1980. Geosynclinal Development of Yenisei Range in Late Precambrian. *Nauka, Moscow*, 70p. (in Russian).
- Powerman, V., Shatsillo, A., Chumakov, N., Kapitonov, I., Hourigan, J., 2015. Interaction between the Central Asian Orogenic Belt (CAOB) and the Siberian craton as recorded by detrital zircon suites from Transbaikalia. *Precamb. Res.* 267, 39–71.
- Rainbird, R.H., Stern, R.A., Khudoley, A.K., Kropachev, A.P., Heaman, L.M., Sukhorukov, V.I., 1998. U-Pb geochronology of Riphean sandstone and gabbro from southeast Siberia and its bearing on the Laurentia-Siberia connection. *Earth Planet. Sci. Lett.* 164, 409–420.
- Rosen, O., 2002. Siberian craton – a fragment of a Paleoproterozoic supercontinent. *Russian J. Earth Sci.* 4, 103–119.

- Rosen, O.M., Turkina, O.M., 2007. Chapter 6.4 The Oldest Rock Assemblages of the Siberian Craton. In: Martin J. van Kranendonk, R.H.S., Vickie, C.B. (Eds.), *Developments in Precambrian Geology*, Elsevier, pp. 793–838.
- Rosen, O., Condie, K.C., Natapov, L.M., Nozhkin, A., 1994. Archean and early proterozoic evolution of the Siberian craton: a preliminary assessment. *Archean Crustal Evol.* 11, 411–459.
- Rosen, O.M., Levskii, L.K., Zhuravlev, D.Z., Rotman, A.Y., Spetsius, Z.V., Makeev, A.F., Zinchuk, N.N., Manakov, A.V., Serenko, V.P., 2006. Paleoproterozoic accretion in the Northeast Siberian craton: isotopic dating of the Anabar collision system. *Stratigr. Geol. Correl.* 14, 581–601.
- Sal'nikova, E.B., Kotov, A.B., Levitskii, V.I., Reznitskii, L.Z., Mel'nikov, A.I., Kozakov, I. K., Kovach, V.P., Barash, I.G., Yakovleva, S.Z., 2007. Age constraints of high-temperature metamorphic events in crystalline complexes of the Irkut block, the Sharyzhalgai ledge of the Siberian platform basement: results of the U-Pb single zircon dating. *Stratigr. Geol. Correl.* 15, 343–358.
- Semikhatov, M.A., Serebryakov, S.N., 1983. *Siberian Hypostratotype of Riphean*. Nauka, Moscow, 223p. (in Russian).
- Semikhatov, M.A., Ovchinnikova, G.V., Gorokhov, I.M., Kuznetsov, A.B., Vasil'eva, I. M., Gorokhovskij, B.M., Podkovyrov, V.N., 2000. Isotopic age of the middle-upper riphean boundary: Pb-Pb geochronology of carbonate rocks, the Lakhanda group, East Siberia. *Doklady Akademii Nauk – Rossijskaya Akademiya Nauk* 372, 216–221 (In Russian).
- Shatsillo, A.V., Kuznetsov, N.B., Pavlov, V.E., Fedonkin, M.A., Priyatkina, N.S., Serov, S. G., Rudko, S.V., 2015. The first magnetostratigraphic data on the stratotype of the Lopata Formation, Northeastern Yenisei Ridge: problems of its age and paleogeography of the Siberian Platform at the Proterozoic-Phanerozoic boundary. *Dokl. Earth Sci.* 465, 1211–1214.
- Shenfil', V.Y. 1991. *Upper Precambrian of the Siberian Platform*. Nauka, Novosibirsk, 206p. (in Russian).
- Smelov, A.P., Kotov, A.B., Sal'nikova, E.B., Kovach, V.P., Beryozkin, V.I., Kravchenko, A. A., Dobretsov, V.N., Velikoslavinskii, S.D., Yakovleva, S.Z., 2012. Age and duration of the formation of the Bilyakh tectonic melange zone, Anabar shield. *Petrology* 20, 286–300.
- Sovetov, Y.K., Komlev, D.A., 2005. Tillites at the base of the Oselok Group, foothills of the Sayan Mountains, and the Vendian lower boundary in the Southwestern Siberian platform. *Stratigr. Geol. Correl.* 13, 337–366.
- Sovetov, J.K., Kulikova, A.E., Medvedev, M.N., 2007. Sedimentary basins in the southwestern Siberian craton: late neoproterozoic-early cambrian rifting and collisional events. *Geol. Soc. Am. Spec. Pap.* 423, 549–578.
- Surkov, V.S., Grishin, M.P., 1997. Structure of Riphean sedimentary basins of the Siberian platform. *Russ. Geol. Geophys.* 38, 1712–1715.
- Turkina, O.M., Nozhkin, A.D., Bayanova, T.B., 2006. Sources and formation conditions of Early Proterozoic granitoids from the southwestern margin of the Siberian craton. *Petrology* 14, 262–283.
- Turkina, O.M., Berezhnaya, N.G., Larionov, A.N., Lepekhina, E.N., Presnyakov, S.L., Saltykova, T.E., 2009. Paleoproterozoic tonalite-trondjemite complex in the northwestern part of the Sharyzhalgai uplift (southwestern Siberian craton): results of U-Pb and Sm-Nd study. *Russ. Geol. Geophys.* 50, 15–28.
- Turkina, O.M., Berezhnaya, N.G., Lepekhina, E.N., Kapitonov, I.N., 2012a. Age of mafic granulites from the early Precambrian metamorphic complex of the Angara-Kan terrain (Southwestern Siberian Craton): U-Pb and Lu-Hf isotope and REE composition of zircon. *Dokl. Earth Sci.* 445, 986–993.
- Turkina, O.M., Berezhnaya, N.G., Lepekhina, E.N., Kapitonov, I.N., 2012b. U-Pb (SHRIMP II), Lu-Hf isotope and trace element geochemistry of zircons from high-grade metamorphic rocks of the Irkut terrane, Sharyzhalgai Uplift: Implications for the Neoproterozoic evolution of the Siberian Craton. *Gondwana Res.* 21, 801–817.
- Turkina, O.M., Kapitonov, I.N., Sergeev, S.A., 2013. The isotope composition of Hf in zircon from Paleoproterozoic plagiogneisses and plagiogranitoids of the Sharyzhalgai uplift (southern Siberian craton): Implications for the continental-crust growth. *Russ. Geol. Geophys.* 54, 272–282.
- Turkina, O.M., Lepekhina, E.N., Berezhnaya, N.G., Kapitonov, I.N., 2014. U-Pb age and Lu-Hf isotope systematics of detrital zircons from paragneiss of the Bulun block (Sharyzhalgai uplift of the Siberian Craton Basement). *Dokl. Earth Sci.* 458, 1265–1272.
- Vernikovskiy, V.A., Vernikovskaya, A.E., Kotov, A.B., Sal'nikova, E.B., Kovach, V.P., 2003. Neoproterozoic accretionary and collisional events on the western margin of the Siberian craton: new geological and geochronological evidence from the Yenisei Ridge. *Tectonophysics* 375, 147–168.
- Vernikovskiy, V.A., Vernikovskaya, A.E., Pease, V.L., Gee, D.G., 2004. Neoproterozoic orogeny along the margins of Siberia. *Geol. Soc. London Memoirs* 30, 233–248.
- Vernikovskiy, V.A., Kazansky, A.Y., Matushkin, N.Y., Metelkin, D.V., Sovetov, J.K., 2009. The geodynamic evolution of the folded framing and the western margin of the Siberian craton in the Neoproterozoic: geological, structural, sedimentological, geochronological, and paleomagnetic data. *Russ. Geol. Geophys.* 50, 380–393.
- Veselovskiy, R.V., Petrov, P.Y., Karpenko, S.F., Kostitsyn, Y.A., Pavlov, V.E., 2006. New Paleomagnetic and isotopic data on the Mesoproterozoic igneous complex on the northern slope of the Anabar uplift. *Dokl. Earth Sci.* 411, 1190–1194.
- Volobuev, M.I., Zykov, S.I., Stupnikova, N.I., 1976. Geochronology of Precambrian formations of the Sayan-Yenisei region of Siberia. In: Vinogradov, A.P. (Ed.), *Topical Problems of the Modern Geochronology*. Nauka, Moscow, pp. 96–123 (in Russian).
- Vrublevich, E.I., 1973. *Geological Map of the USSR. Scale 1: 200000. Ser. Yenisei. Sheet P-46-XXVI. Aerogeology*. (in Russian).
- Wiedenbeck, M., Allé, P., Corfu, F., Griffin, W.L., Meier, M., Oberli, F., Quadt, A.V., Roddick, J.C., Spiegel, W., 1995. Three natural zircon standards for U-Th-Pb, Lu-Hf, trace element and REE analysis. *Geostand. Newslett.* 19 (1), 1–23.